

**UCSF**

**UC San Francisco Electronic Theses and Dissertations**

**Title**

Prion-Like Characteristics of the Microtubule-Associated Protein Tau

**Permalink**

<https://escholarship.org/uc/item/9c84v3s2>

**Author**

Frost, Susan Elizabeth

**Publication Date**

2009

Peer reviewed|Thesis/dissertation

**PRION-LIKE CHARACTERISTICS OF THE  
MICROTUBULE-ASSOCIATED PROTEIN TAU**

by

Susan "Bess" Frost

DISSERTATION

Submitted in partial satisfaction of the requirements for the degree of

DOCTOR OF PHILOSOPHY

in

BIOMEDICAL SCIENCES

in the

GRADUATE DIVISION

of the

UNIVERSITY OF CALIFORNIA, SAN FRANCISCO

**Copyright 2009  
by  
Susan Frost**

for my grandmother

*Dr. Marianna Frost*

& my mother

*Dr. Diane Davis-Frost*



## ACKNOWLEDGEMENTS

There are many people who deserve a tremendous amount of thanks upon completion of my dissertation. My family has a tradition of lifelong learning, and has been a constant source of strength and support throughout my life. My parents have unwavering faith in my decisions and abilities. I thank my husband, Erik Hunter, for encouragement, tolerance, and a three-dimensional tau video. He has been instrumental to my sanity and happiness as a graduate student.

My success at UCSF was greatly influenced by the exceptional guidance of my advisor, Dr. Marc Diamond, who imparted guided freedom throughout the duration of my training. The amount of time he devotes to members of his lab is unprecedented, and pays off in productivity. Marc has been a reliably strong advocate for me, and I look forward to working with him throughout my scientific career.

The Diamond lab is a delightful environment, filled with curious and inquisitive people. I would especially like to thank Suzanne Angeli, Rachel Jacks and Kiriko Masuno, whose friendship, humor, and commiseration made the rejections and revisions tolerable.

I would also like to thank my committee members, Dr. Jonathan Weissman and Dr. Paul Muchowski. Additional thanks goes to Dr. Weissman for use of his atomic force microscope, Dr. Brian Shoichet. for use of his JASCO spectrophotometer, Kurt Thorn and the NIKON center for use of their confocal microscope, Dr. Virginia Lee for the

pRK172 vector, and Dr. Tony Gerber for the mCherry vector.

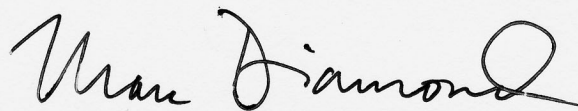
This work was supported by grants from the Sandler Family Supporting Foundation, the Taube Family Foundation Program in Huntington's Disease Research, the Muscular Dystrophy Association, and NINDS:R01 NS50284-03 (M.I.D.), and an NIH Training Grant for Neurodegenerative Diseases (S.F.).

# PRION-LIKE CHARACTERISTICS OF THE MICROTUBULE-ASSOCIATED PROTEIN TAU

Susan “Bess” Frost

Tauopathies are neurodegenerative diseases characterized by neurofibrillary tangles and/or paired helical filaments of the microtubule-associated protein tau in neurons and glia. While most protein misfolding diseases present with a well-defined pathological syndrome that is restricted to specific subsets of neurons, tau pathology is associated with many distinct disease phenotypes. Furthermore, in Alzheimer disease, tau pathology appears to spread inexorably through the central nervous system along neuroanatomical connections. These features are reminiscent of prion diseases, which exhibit considerable phenotypic diversity and spread pathology between tissues and among individuals. Based on Fourier-transform infrared spectroscopy, circular dichroism, fragility, and electron microscopy, wild-type tau can exist in two self-propagating conformations *in vitro* with distinct secondary structures, strengths, and morphologies that arise via templated conformation change. In addition, tau aggregates, but not monomer, enter cultured C17.2 neural precursor cells and stimulate fibrillization of intracellular tau. When purified from cells, these fibrils are competent to propagate fibrillization *in vitro*, and the newly aggregated intracellular tau is capable of traveling between co-cultured cells. The prion-like characteristics of tau are relevant to two key features of tauopathy: phenotypic diversity of the sporadic and inherited tauopathies induced by distinct tau conformers, and spread of disease through the brain. They suggest

a general pathogenic mechanism for other neurodegenerative diseases linked to fibrillar protein aggregation.

A handwritten signature in black ink that reads "Marc I. Diamond". The signature is written in a cursive style with a large, prominent "D" at the end.

---

Marc I. Diamond, M.D.

Thesis Advisor

## CONTRIBUTIONS

Portions of the text and figures presented in this thesis are reproduced with permission from material published previously. Chapter 2 “Conformational Diversity of Wild-Type Fibrils Specified by Templated Conformation Change” was published in February 2009 in the *Journal of Biological Chemistry*, Vol. 284(6), pp. 3546-51. Dr. Julian Ollesch performed the Fourier-transform infrared spectroscopy (FTIR) (Fig. 3, 4), and Dr. Holger Wille performed electron microscopy (Fig. 8).

Chapter 3 “Extracellular to Intracellular Propagation of Tau Misfolding” was published in March 2009 in the *Journal of Biological Chemistry*. Rachel Jacks conducted the experiment in which cells were co-treated with tau and dextran (Fig. 5).

Aside from these items, the work presented in this thesis was conducted by its author, Susan “Bess” Frost, under the supervision of Dr. Marc Diamond.

## PERMISSION TO REPRINT

It is the policy of the Journal of Biological Chemistry that it is free to copy, distribute, transmit and to adapt the work under the following conditions: 1) the work must be attributed in the manner specified by the original source, and 2) the work may not be used for commercial purposes.

It is the policy of Landes Bioscience/Eurekah, publisher of the journal Prion, that authors have the non-exclusive right to use of all or part of the contribution in any book or article written by the author, including doctoral theses. As a condition for this license to the author, all such books and articles containing the contribution or any part thereof must include the copyright notice that appears on the issue of the journal in which the contribution is first published and a full citation of the journal.

# TABLE OF CONTENTS

<b>Preface</b>	Acknowledgements	<b>iv</b>
	Abstract	<b>vi</b>
	Contributions	<b>viii</b>
	Permission to Reprint	<b>ix</b>
	Table of Contents	<b>x</b>
	List of Figures	<b>xi</b>
<b>Chapter 1</b>	Introduction	<b>1</b>
<b>Chapter 2</b>	Conformational Diversity of Wild-Type Fibrils Specified by Templated Conformation Change	<b>6</b>
<b>Chapter 3</b>	Extracellular to Intracellular Propagation of Tau Misfolding	<b>31</b>
<b>Chapter 4</b>	The Expanding Realm of Prion Phenomena in Neurodegenerative Disease	<b>60</b>
<b>Chapter 5</b>	Conclusions and Future Directions	<b>74</b>
<b>Appendix A</b>	References	<b>77</b>

## LIST OF FIGURES

### Chapter 2

<b>Figure 1</b>	Schematic for fibril seeding	<b>16</b>
<b>Figure 2</b>	Kinetics of fibril seeding	<b>17</b>
<b>Figure 3</b>	FTIR analysis of WT, MUT, and WT* tau	<b>19</b>
<b>Figure 4</b>	Quantification of FTIR analysis of WT, MUT, and WT* tau	<b>20</b>
<b>Figure 5</b>	CD analysis of WT, MUT, and WT* tau fibrils	<b>22</b>
<b>Figure 6</b>	WT fibrils are more fragile than MUT and WT* fibrils based on AFM	<b>24</b>
<b>Figure 7</b>	WT fibrils are more fragile than MUT and WT* fibrils based on CD	<b>25</b>
<b>Figure 8</b>	Negative stain electron microscopy of tau fibrils	<b>27</b>
<b>Figure 9</b>	$\Delta$ K280 seeds a novel type of WT fibril conformation, WT <sup>K</sup>	<b>30</b>

### Chapter 3

<b>Figure 1</b>	Tau constructs	<b>41</b>
<b>Figure 2</b>	Full-length tau-YFP binds microtubules while MTBR-YFP aggregates in C17.2 neural cells	<b>42</b>
<b>Figure 3</b>	Tau aggregates are sensitive to trypsin	<b>45</b>
<b>Figure 4</b>	C17.2 cells take up aggregated tau	<b>46</b>



<b>Figure 5</b>	Extracellularly-derived aggregates co-localize with a marker of endocytosis	48
<b>Figure 6</b>	Extracellular tau enters cells and induces aggregation of full-length tau-YFP in cultured cells based on biochemistry	50
<b>Figure 7</b>	Extracellular tau enters cells and induces aggregation of full-length tau-YFP in HEK293 and C17.2 cells	52
<b>Figure 8</b>	Induced tau-YFP aggregates in C17.2 cells are fibrillar and seed MTBR fibrillization <i>in vitro</i>	54
<b>Figure 9</b>	MTBR-YFP aggregates transfer between co-cultured cells	56
<b>Figure 10</b>	Tau-YFP aggregates transfer between co-cultured cells	57

# **CHAPTER 1**

## **INTRODUCTION**

## **Introduction**

In 1907, German physician and scientist Alois Alzheimer described the brain of his patient Auguste Deter (Alzheimer 1907). The two pathological hallmarks he observed were “numerous small miliary foci” and “tangled bundles of fibrils.” The foci, or “plaques,” were observed extracellularly, while the tangles were observed both inside and outside of cells. Many decades later, the components of these plaques and tangles were identified.  $\beta$ -amyloid made up the plaques (Masters et al. 1985), and tau, a protein normally responsible for binding, stabilizing, and promoting the polymerization of neuronal microtubules (Weingarten et al. 1975), composed the tangles (Kosik et al. 1986). Extracellular tau aggregates were later referred to as “tombstone” or “ghost” tangles (Braak et al. 1994), because they appeared to be remnants of dead cells.

Genetic linkage implicates  $A\beta$  pathology as a causal factor for Alzheimer disease (AD) (Levy et al. 1990; Van Broeckhoven et al. 1990). Mutations in the amyloid precursor protein (APP) or presenilins (Sherrington et al. 1995) cause early-onset Alzheimer disease, though 90% of AD occurs sporadically. Presenilin 1 and 2 are components of a complex that cleaves APP to produce  $A\beta$  (Wolfe et al. 1999). Despite genetic association, tau tangles, not  $A\beta$  plaques, correlate with disease severity and are locally co-incident with neuronal death (Braak et al. 1991). Strikingly, tau aggregation is involved in over twenty other neurodegenerative diseases, termed “tauopathies,” 10% of which are due to mutations in the tau gene (Delacourte 2005). Since neurodegeneration is not observed in the absence of tau in AD mouse models, an emerging theory is that  $A\beta$  initiates AD, and that tau is a downstream effector of degeneration (Roberson et al.

2007). Nevertheless, many therapies have been developed that target A $\beta$  aggregation, modulate soluble levels of A $\beta$ , or block cleavage of APP (Rafii et al. 2009). Less attention has been paid to targeting tau, yet therapies targeting tau hyperphosphorylation and aggregation are beginning to be investigated (Rafii et al. 2009). Despite extensive research, there is no effective disease-modifying treatment available for AD.

### **Diversity of Disease Phenotypes**

Tauopathies are neurodegenerative diseases characterized by neuronal and glial neurofibrillary tangles and/or paired helical filaments composed of the microtubule-associated protein tau (MAPT). Mutations in the tau gene cause frontotemporal dementia with parkinsonism linked to chromosome 17 (FTDP-17) (Hutton et al. 1998; Poorkaj et al. 1998; Spillantini, Murrell et al. 1998). Among the tauopathies, there is considerable variation in the localization of neurodegeneration, cell types affected (neurons and/or glia), age of onset, and duration of disease (Delacourte 2005). It is unknown how the pathology of one protein can generate distinct pathological syndromes. It is possible that the clinical variability in sporadic tauopathies could be due to distinct rates of tau fibril formation and propagation that arises from different tau conformations, as has been described as the “strain phenomenon” for prion proteins (Bessen et al. 1995; Telling et al. 1996; Prusiner 1997).

The unstructured nature of soluble tau protein makes it highly flexible, similar to other aggregation-prone proteins, and could make it especially prone to misfolding

stimulated by mutant tau or other amyloid seeds. Indeed,  $\alpha$ -synuclein can seed tau fibrillization (Giasson et al. 2003), and fibrillar tau seeds increase the rate of tau fibrillization (Friedhoff et al. 1998). Taking clues from prion biology, we hypothesized that wild-type tau adopts pathologically distinct conformations that give rise to phenotypically distinct diseases. We found that wild-type tau is capable of conformational diversity which is generated through templated conformation change (Frost, Ollesch et al. 2009).

### **Pathological Spread**

The spread of neurodegeneration presents a fascinating question: Why does pathology often occur in anatomically and functionally interconnected groups of cells? For example, in amyotrophic lateral sclerosis, the spread of disease through adjacent regions of the spinal cord is well described (Cudkowicz et al. 2004). In this motor neuron disease, one muscle group is affected, and then contralateral and adjacent muscle groups are affected. Tauopathies are also temporally and neuroanatomically progressive. The distribution of tau aggregates is consistent with the hierarchies of cortico-cortical connections in AD brains, and cortical vulnerability shares a close correlation with trans-synaptic distance from the affected areas (Arnold et al. 1991). The first cells affected are the glutamatergic projection cells of the transentorhinal region. Pathology then extends to the entorhinal region proper, affecting the hippocampal formation, amygdala, and then the higher order multimodal association areas of the neocortex. Degeneration can then be detected in the primary motor area and primary sensory fields. The disease culminates in

extensive damage of the neocortex, from which lesions spread superolaterally from the inferior temporal areas (Braak et al. 1997). Progressive supranuclear palsy also exhibits pathological tau spreading, though the cell types and affected brain areas differ (Delacourte 2005). The spread of pathology from region to adjacent region along trans-cortical connections is reminiscent of a domino effect: the damage in one cell leads to damage of the downstream cell, and so on.

One intriguing possibility for the evolution of neurodegenerative diseases within the central nervous system (CNS) is that misfolded or aggregated proteins gain entry to connected cells. There is now growing evidence to support this idea for prion diseases and other protein misfolding disorders. Several types of amyloid proteins are capable of membrane permeabilization and cell entry. Extracellular prion proteins and A $\beta$  gain entry into cells (Magalhaes et al. 2005), and prion infectivity transfers between cells within close proximity or direct contact (Kanu et al. 2002). Prions also travel from cell to cell in exosomes (Fevrier et al. 2004) and tunneling nanotubes (Gousset et al. 2009). Aggregated polyglutamine proteins are taken up by cells, and stimulate aggregation of intracellular polyglutamine (Ren et al. 2009). Soluble oligomers of several different amyloid proteins increase lipid bilayer conductance, regardless of sequence (Kayed et al. 2004), thus it has been proposed that membrane permeabilization is not unique to the prion protein, and rather is a common, conformation-based property of all amyloid proteins. We have found that extracellular tau aggregates are taken up by cells and stimulate intracellular tau fibrillization, aggregates of which transfer between co-cultured cells (Frost, Jacks et al. 2009).

## **Summary**

Tauopathies represent a varied group of neurodegenerative diseases, yet existing research has not clearly explained how tau misfolding contributes to phenotypic diversity. Moreover, it is unclear why many neurodegenerative diseases, including tauopathy, spread inexorably through the nervous system, whereas others remain largely confined to specific neuronal subgroups. In chapter 2, we show that wild-type tau fibrils exhibit self-propagating conformational change. In chapter 3, we show that tau aggregates transfer from the extracellular to intracellular space, where they stimulate aggregation of intracellular tau, which transfers between co-cultured cells. In chapter 4, we discuss emerging principles of amyloid-based neurodegeneration, and similarities between non-infectious neurodegenerative diseases and prion diseases. Based on similarities between tau and prion biology, we hypothesize that different tau conformers may underlie the phenotypic diversity of sporadic tauopathies, and that tau seeds spread from cell to cell along neural networks in the brain. Our experiments lay the groundwork to test this hypothesis. If confirmed in animal models, this data may have broad implications for understanding and treating a variety of amyloid-associated neurodegenerative diseases.

## **CHAPTER 2**

# **CONFORMATIONAL DIVERSITY OF WILD-TYPE TAU FIBRILS SPECIFIED BY TEMPLATED CONFORMATION CHANGE**



# **Conformational Diversity of Wild-Type Tau Fibrils Specified by Templated Conformation Change**

Bess Frost<sup>1,2,3</sup>, Julian Ollesch<sup>4</sup>, Holger Wille<sup>1,4</sup>, and Marc I. Diamond<sup>1,2,3,4</sup>

From Departments of <sup>1</sup>Neurology, and <sup>2</sup>Cellular and Molecular Pharmacology,  
<sup>3</sup>Biomedical Sciences Program, and <sup>4</sup>Institute for Neurodegenerative Diseases  
University of California, San Francisco  
1600 16<sup>th</sup> St.  
San Francisco, CA  
Email: [marc.diamond@ucsf.edu](mailto:marc.diamond@ucsf.edu)

[Reprinted from Journal of Biological Chemistry, Vol 284(6), pp. 3546-51]

## **Abstract**

Tauopathies are sporadic and genetic neurodegenerative diseases characterized by aggregation of the microtubule-associated protein tau. Tau pathology occurs in over twenty phenotypically distinct neurodegenerative diseases, including Alzheimer disease and frontotemporal dementia. The molecular basis of this diversity among sporadic tauopathies is unknown, but distinct fibrillar wild-type tau conformations could play a role. Using Fourier-transform infrared spectroscopy, circular dichroism, and electron microscopy, we show that wild-type (WT) tau fibrils and P301L/V337M (MUT) tau fibrils have distinct secondary structures, fragilities, and morphologies. Furthermore, MUT fibrillar seeds induce WT tau monomer to form a novel fibrillar conformation, termed WT\*, that is maintained over multiple seeding reactions. WT\* has secondary structure, fragility, and morphology that is similar to MUT fibrils and distinct from WT fibrils. WT tau is thus capable of conformational diversity that arises via templated conformation change, as has been described for A $\beta$ ,  $\beta$ 2-microglobulin, and prion proteins.

## Introduction

Tau filament deposition in Alzheimer disease (AD), frontotemporal dementia, and other tauopathies correlates closely with cognitive dysfunction and cell death (Braak et al. 1991). About 10% of tauopathies are due to dominant mutations in the tau gene. These diseases are collectively termed frontotemporal dementia with parkinsonism linked to chromosome 17, FTDP-17 (Hutton et al. 1998; Poorkaj et al. 1998; Spillantini, Murrell et al. 1998). Most of the mutations occur in the microtubule-binding region (MTBR) of the tau protein, which is thought to be both its functional (Lewis et al. 1988) and pathogenic (Wischik et al. 1988) “core.” Approximately 90% of tauopathies occur sporadically, and involve only WT tau. Both familial and sporadic tauopathies vary by regional involvement, disease duration, age of onset, tau isoform expression, and fibril morphology (Buee et al. 2000). It is unknown how the pathology of WT tau might generate distinct disease phenotypes in sporadic tauopathies, and whether conformational diversity of the protein could potentially play a role in disease, as it does in prion disorders (Tanaka et al. 2004; Legname et al. 2006).

Mutations in the tau gene can generate conformationally distinct tau species. Structural differences between *in vitro* prepared WT, G272V, N279K, P301L, V337M and  $\Delta$ K280 tau fibrils have been observed using Fourier-transform infrared spectroscopy (FTIR) (von Bergen et al. 2000), and differential susceptibilities to protease cleavage *in vitro* have been described for WT and P301L tau fibrils (Aoyagi et al. 2007). Furthermore, tau filaments extracted from diseased brain are often morphologically

distinct, consisting of straight or paired helical filaments of various periodicities and widths (Crowther et al. 2000). It is unknown whether WT tau can assume self-propagating, structurally distinct fibrillar conformations, as has been described for A $\beta$  peptide (Petkova et al. 2005),  $\beta$ 2-microglobulin (Yamaguchi et al. 2005), and the prion protein (Bessen et al. 1995). In this study, we have used biochemical and biophysical methods to test the hypothesis that WT tau fibrils exhibit conformational diversity that is maintained by templated conformation change.

## Experimental Procedures

***Tau Expression and Purification.*** The MTBR (amino acids 243 to 375 of the 441 amino acid tau isoform) of WT tau and the P301L/V337M tau double mutation (MUT) used in all fibrillization reactions were subcloned into pRK172. Recombinant tau MTBR was prepared as described previously from Rosetta (DE3)pLacI competent cells (Novagen), exploiting the heat stability of tau protein followed by cation exchange chromatography (Goedert et al. 1990). Single-use aliquots were stored at -80 °C in 10 mM HEPES and 100 mM NaCl (pH 7.4).

***Tau Fibrillization and Seeding Assays.*** 4  $\mu$ M tau monomer was incubated for indicated times at room temperature without agitation in 5 mM DTT, 10 mM HEPES (pH 7.4), 100 mM NaCl, and 150  $\mu$ M arachidonic acid (Wilson et al. 1995) (Sigma-Aldrich). Tau appears in the insoluble fraction after a 15 h fibrillization reaction and 100,000 x g ultracentrifugation. Alternatively, seeded reactions were carried out using a 10% aliquot from a fibrillization reaction (i.e. 0.4  $\mu$ M total tau protein) and 4.0  $\mu$ M monomer in three successive incubations. The primary (1°) fibrillization reaction was initiated with 150  $\mu$ M arachidonic acid. After 15 h, the secondary (2°) fibrillization was initiated by exposure of 4.0  $\mu$ M monomer to 10% of the 1° reaction. After 3 h, the tertiary (3°) reaction was initiated by exposure of 4.0  $\mu$ M monomer to 10% of the 2° reaction. After 3 h, the quaternary (4°) reaction was initiated by exposure of 4.0  $\mu$ M monomer to 10% of the 3° reaction, resulting in a 1,000 fold dilution of the 1° seed. The 4° reaction was allowed to proceed for 96 h before further analysis. WT\* was produced by using 1° MUT tau as a seed for WT monomer in serial seeding reactions (MUT seed WT seed WT seed WT).

**Thioflavin T.** When measuring fibrillization rate of 1° reactions, 12.5  $\mu$ M thioflavin T (ThT; Sigma-Aldrich) was included in the reaction (LeVine 1993). Measurements were recorded at 455 excitation/485 emission in a Safire plate reader (Tecan) every 10 min for 1 h, and every 30 min for the next 14 h. When measuring fibrillization rate of 4° reactions, 12.5 mM ThT was mixed with aliquots of the 4° reaction every 24 h and measured as described.

**Fourier Transform Infrared Spectroscopy.** WT and MUT tau fibrils were polymerized through serially seeded reactions as described. The polymerized tau from 4° reactions was pelleted by ultracentrifugation, resuspended in water, and lyophilized for 48 h. The lyophilisates were resuspended in D<sub>2</sub>O. Infrared absorbance spectra were recorded against pure D<sub>2</sub>O. Buffers and salts did not interfere with the amide I absorption band (1700-1600  $\text{cm}^{-1}$ ). For each sample, 64 double-sided interferograms were scanned bidirectionally and averaged on a Perkin Elmer System 2000 FTIR spectrometer, equipped with an MCT detector and purged with dry N<sub>2</sub>. Spectra were recorded with a 2  $\text{cm}^{-1}$  instrument resolution, and 4-fold zero-filling yielded one data point per 0.5  $\text{cm}^{-1}$ . Trace signals from water vapor were eliminated with the suppression algorithm of the software SpectrumGX V5 (Perkin Elmer). Additionally, low frequency noise was filtered with a Fourier self-deconvolution algorithm at 8-10  $\text{cm}^{-1}$  cut-off as necessary, and the amide I band was baseline corrected. Secondary structure information was derived by amide I band decomposition as described previously (Ollesch et al. 2007). Cauchy curves were numerically determined to add up to the shape of the amide I band. The Cauchy

curve integrals were used to calculate the fraction of secondary structure that is assigned to the peak frequency of the curve. Curve fitting all amide I bands with identical initialization parameters for the number of bands, band position, width, shape, and the automatic determination of each intensity as well as the overall baseline values resulted in a high sensitivity for structural changes. The secondary structure fractions presented in Fig. 4 were averaged from six spectra (MUT aggregate from five) of two separate aggregation assays. Thereby we were able to suppress the negative effects of residual water vapor, and to quantify the quality of our analysis with the error bars presented.

**Circular Dichroism.** 1° and 4° reactions were ultracentrifuged at 100,000 x g for 1 h at room temperature, and pellets were resuspended in PBS to a final concentration of approximately 4.0 μM prior to circular dichroism (CD). Spectra were recorded on a JASCO spectrometer. Spectra reflect four accumulations.

**Atomic Force Microscopy.** Reactions were adsorbed onto mica chips (Ted Pella, Inc.) for 2 min, washed twice with 200 μl water, and allowed to dry for at least 1 h prior to tapping mode atomic force microscopy (AFM) (Veeco).

**Fiber Fragility Assays.** Whole 1° and 4° fibrillization reactions of WT, MUT, and WT\* were dialysed into PBS for 15 h. CD spectra were measured from 250 to 200 nm, after which the reactions were sonicated with a titanium probe on a Branson Sonifier 250 (Danbury, CT) at 50% duty and 10% intensity for 1 min, and CD spectra were again measured. The changes in WT, MUT, and WT\* signals were compared using Wilcoxon

signed rank statistical analysis in fragility assays. The data set (n=6) presented meets all requirements for this type of one sided, two-tailed nonparametric analysis.  $\alpha < .025$ ,  $p = .0156$  for all fragility assays.

**Electron Microscopy.** 4° fibrillization reactions were adsorbed onto glow-discharged formvar/carbon copper grids (200 mesh, Ted Pella, Inc.). The grids were washed with ammonium acetate buffer, stained with uranyl acetate, dried, and viewed in a FEI Tecnai F20 electron microscope (EM) at 80 kV and a standard magnification of 25,000 (Wille et al. 2007). Electron micrographs were recorded with a Gatan Ultrascan CCD camera. The magnification was calibrated using negatively stained catalase crystals and ferritin. The percentage of paired helical filaments were compared between WT, MUT, and WT\* 4° reactions using the Student's t-test. The data set (n=3) presented meets all requirements for this type of two-tailed two-sample equal variance analysis.  $*=p < 10^{-5}$ .



## Results

### Fibril Seeding Strategy

We established a protocol to create pools of fibrillar protein under uniform conditions (Fig. 1A, B). The 1° WT and MUT fibrillization reactions were induced by arachidonic acid (Wilson et al. 1995). The 2° reaction was a seeded reaction, in which 4.0  $\mu$ M monomer was incubated with 10% of the 1° reaction in the absence of arachidonic acid for 3 h. The 2° seeding reaction was followed by two additional seeding reactions to produce the 3° and 4° reactions (Fig. 1A). To induce a novel fibrillar conformation of WT tau, termed WT\*, we performed a cross-seeding reaction in which the 1° MUT reaction was incubated with WT monomer. Three serial seeding reactions were then performed using WT monomer (Fig. 1B). After 96 h, 4° reactions were ultracentrifuged and the insoluble fractions were compared using FTIR, CD, and EM. Whole reactions were compared for fragility assays. We first determined the extent of fibrillization and the fibrillization rate for each reaction. In 1° reactions, 81% of WT monomer and 89% of MUT monomer is present in the insoluble fraction after 15 h (Fig. 2A, B), indicating that most of the protein is in an aggregated form. 1° WT and MUT reactions have similar rates of fibrillization based on ThT fluorescence (LeVine 1993) (Fig. 2C). In 4° seeded reactions, WT and WT\* also have similar degrees of aggregation. 22% of WT and 21% of WT\* 4° reactions are insoluble after 96 h (Fig. 2D, E). Monitoring ThT fluorescence of the 4° reactions produced a  $t_{1/2}$  of 24 h for WT, 18 h for MUT, and 13 h for WT\* (Fig. 2F). Despite different  $t_{1/2}$  values, all reactions reach a plateau by about 48 h.

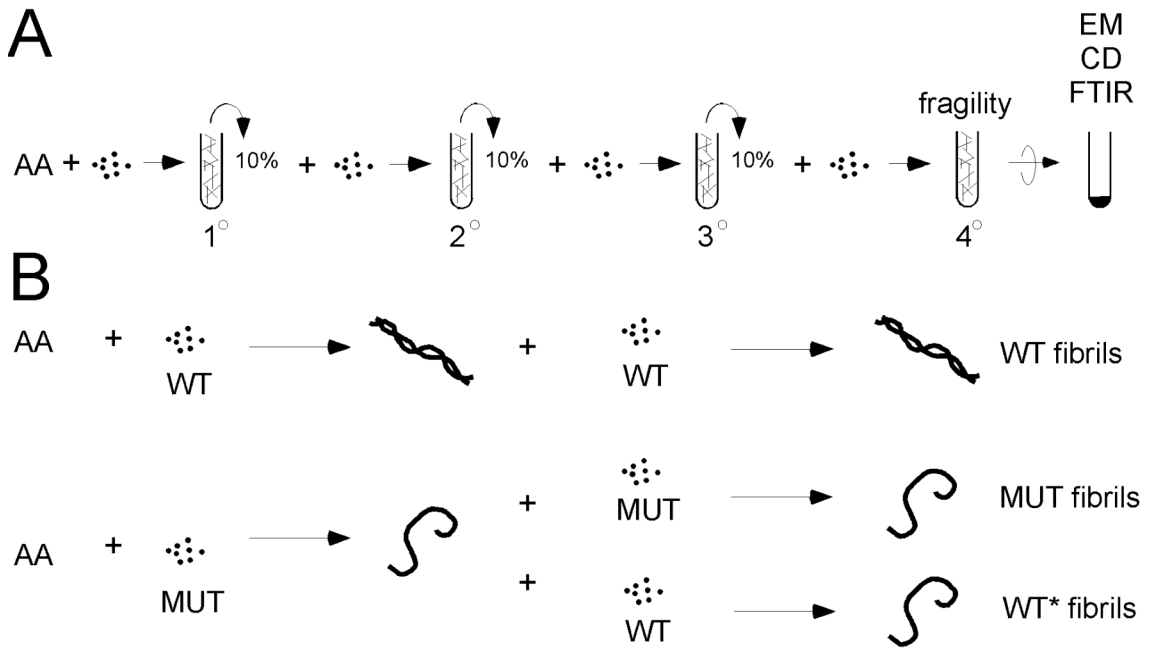


Figure 1: Schematic for fibril seeding

(A) Arachidonic acid is used to stimulate monomer fibrillization in the  $1^\circ$  reaction. In the  $2^\circ$  reaction, 10% of the  $1^\circ$  reaction is used to seed the fibrillization of tau monomer. In the  $3^\circ$  reaction, 10% of the  $2^\circ$  reaction is used to see the fibrillization of tau monomer. In the  $4^\circ$  reaction, 10% of the 3 reaction is used to seed the fibrillization of tau monomer. For fragility studies, the whole  $4^\circ$  reaction was used, uncentrifuged. For FTIR, CD, and EM, the  $4^\circ$  reaction was ultracentrifuged for 1 h at 100,000 x g, and the pellet was used for measurements.

(B) Arachidonic acid is used to stimulate WT or MUT fibrillization in the  $1^\circ$  reaction. To generate WT fibrils, 10% of the  $1^\circ$  WT reaction is incubated with WT monomer, followed by three serial seeding reactions as described in (A). To generate MUT fibrils, 10% of the  $1^\circ$  MUT reaction is incubated with MUT monomer, followed by three serial seeding reactions as described in (A). To generate WT\* fibrils, 10% of the  $1^\circ$  MUT reaction is incubated with WT monomer, followed by three serial seeding reactions as described in (A).

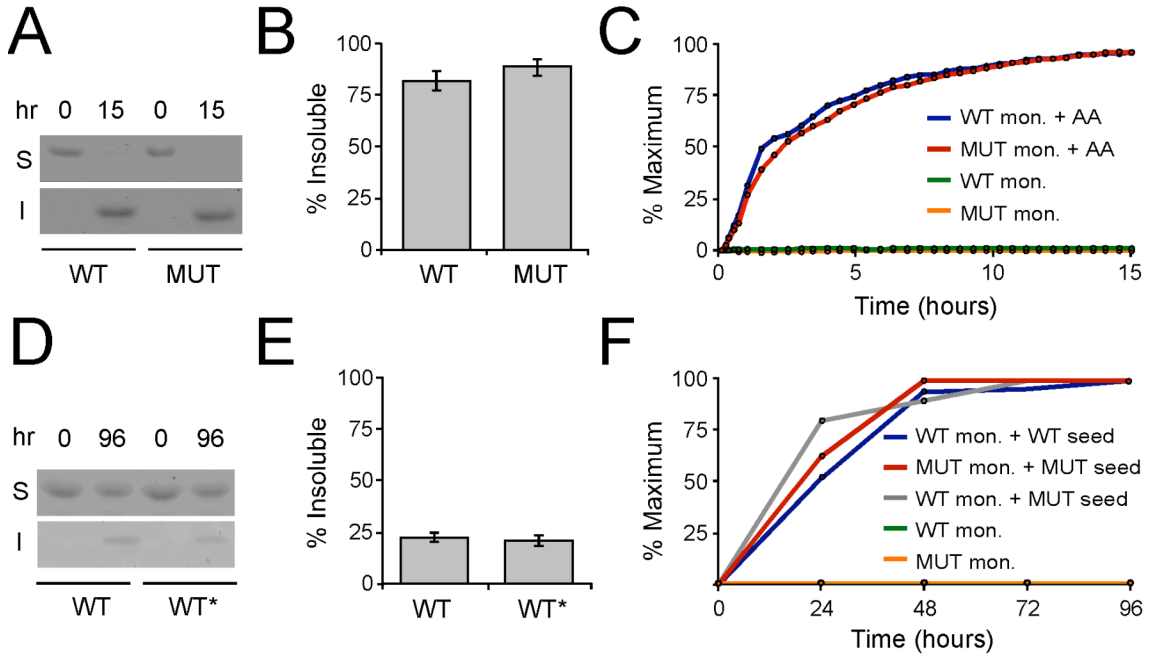


Figure 2: Kinetics of fibril seeding

- (A) After 15 h, 1° WT and MUT have comparable degrees of fibrillization as determined by solubility. 1° reactions were ultracentrifuged for 1 h at 100,000 x g. The (S) soluble and (I) insoluble fractions were compared by Coomassie stain.
- (B) Quantification of three separate experiments: after 15 h, 81% of WT tau monomer is insoluble, versus 89% of MUT tau, indicating comparable degrees of fibrillization.
- (C) 1° WT and MUT fibrillization reactions were initiated with arachidonic acid, and measured over time using ThT fluorescence at 455ex/485em. Both reactions proceeded at a similar rate.
- (D) After 96 h, WT and WT\* 4° reactions have comparable degrees of fibrillization. 4° reactions were ultracentrifuged for 1 h at 100,000 x g. The (S) soluble and (I) insoluble fractions were compared by Coomassie stain.
- (E) Quantification of three separate experiments: after 96 h, 22% of WT tau monomer is insoluble, versus 21% of WT\* tau, indicating comparable degrees of fibrillization.
- (F) WT monomer, MUT monomer, WT, MUT, and WT\* 4° reactions were monitored for 96 h using ThT fluorescence at 455ex/485em. The  $t_{1/2}$  values for WT, MUT, and WT\* were 24 h, 18 h, and 13 h, respectively. All reactions reach a plateau by approximately 48 h.

## **WT and WT\* fibrils have different secondary structures based on Fourier-transform infrared spectroscopy**

We used FTIR to compare monomer and 4° fibril structures. The applied data processing is extremely sensitive for structural differences, which enabled a detailed comparison of the selected tau conformations. WT and MUT monomer showed no appreciable differences in secondary structure (Fig. 3A, B, Fig. 4). In contrast, 4° WT and MUT tau fibrils exhibited distinct FTIR spectra. WT tau had relatively more heterogeneity in signal, partially due to lower signal intensity, but also possibly representing a larger diversity of structures, whereas MUT tau was quite homogeneous (Fig. 3C, D). Spectral deconvolution indicated that, with a significance level of 5.0% in a Student's t-test, WT fibrils contained significantly more  $\alpha$ -helix, significantly less  $\beta$ -sheet, and relatively less  $\beta$ -turn than MUT (Fig. 4). Likewise, 4° WT\* spectra were clearly distinct from WT, with significantly less  $\alpha$ -helical and apparently greater random coil content (Fig. 3E, Fig. 4). The absolute values for the secondary structure fractions are only estimates (approximately  $\pm 10$ -15%), since a structural template for calibration of tau secondary structure analysis (Ollesch et al. 2007) does not exist. Still, the applied method is highly sensitive for spectral differences between samples of a similar origin (Hofmann et al. 2004; Ollesch et al. 2007; Ollesch et al. 2008). Thus, although we cannot define with absolute assurance the structure of the fibrils, FTIR spectral differences between WT and WT\* fibrils are clear.

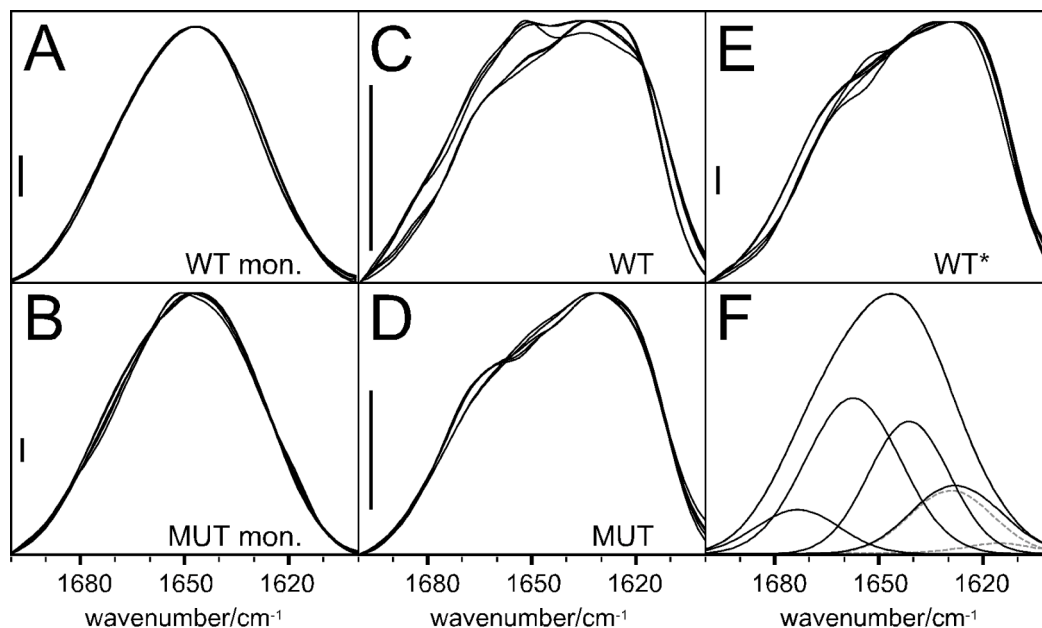


Figure 3: FTIR analysis of WT, MUT, and WT\* tau

- (A) WT monomer.
- (B) MUT monomer.
- (C) 4° WT, (D) 4° MUT and (E) 4° WT\* aggregates prepared as described for FTIR. (D) MUT and (E) WT\* exhibit distinct spectra from (C) WT. (E) WT\* aggregates exhibit a redshift of the amide I maximum to 1630  $\text{cm}^{-1}$  compared with WT aggregates (approx. 1634  $\text{cm}^{-1}$ ) and MUT aggregates (1632  $\text{cm}^{-1}$ ).
- (F) A curve fit example demonstrates the achieved accuracy (the calculated sum of band components superimposes the measured amide I band completely), and the fiber component bands used. They describe (high to low wavenumber)  $\beta$ -turns,  $\alpha$ -helix, random coil, and  $\beta$ -sheet. For  $\beta$ -sheet, a high- and a low-frequency band were assumed (dashed lines). In (A), (B), (C), (E), six spectra from two preparations are superimposed, five are superimposed in (D). The main reasons for the large variability of the spectra between 1665-1645  $\text{cm}^{-1}$  were residual water vapor and a low protein concentration in the samples, especially of WT fibrils. Scale bars represent  $5 \times 10^{-3}$  arbitrary units.

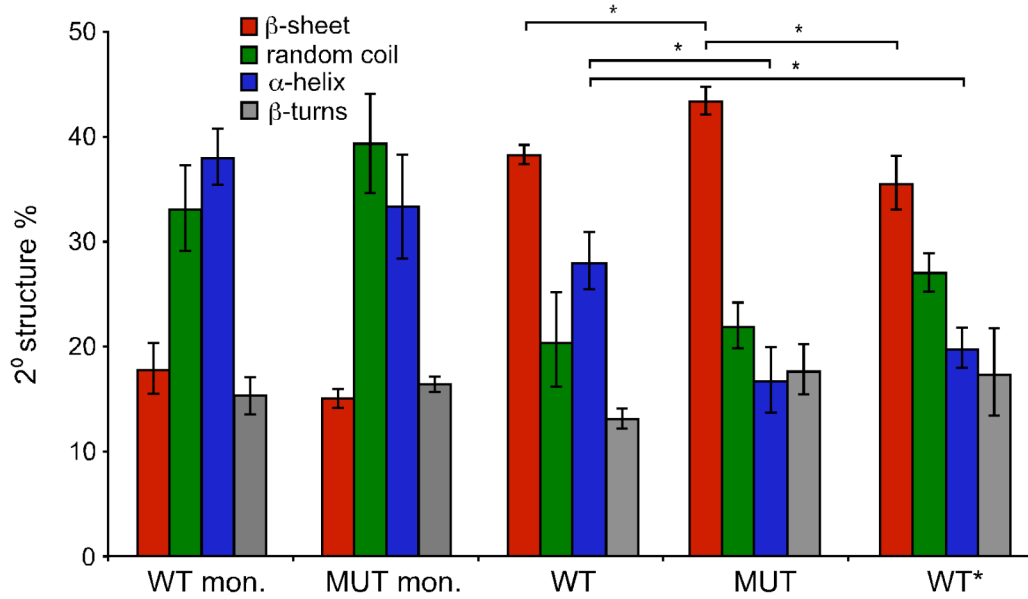


Figure 4: Quantification of FTIR analysis of WT, MUT, and WT\* tau

Quantification of Figure 3. The results presented derive from curve fitting and averaging six spectra of two samples for each condition. Error bar represent the S.E.M. \*= $p < .05$ .

### **WT and WT\* fibrils have distinct secondary structures based on circular dichroism**

To extend the FTIR studies, we used CD spectroscopy to compare WT, MUT, and WT\* fibrils. We prepared 1° reactions as described. After 15 h, we ultracentrifuged the reactions and resuspended the pellets in PBS. The MUT minimum occurs at about 218 nm, versus 223 nm for WT fibrils (Fig. 5A). These minima indicate that MUT fibrils contain more  $\beta$ -sheet structure than WT fibrils, and WT fibrils contain more  $\alpha$ -helix, which is consistent with data obtained from FTIR. The minimum for MUT fibrils was also consistently deeper than that of WT fibrils. We then compared CD spectra of 4° WT and WT\* reactions, prepared as described previously, again measuring only the insoluble material. The CD spectrum of 4° WT\* was clearly different from 4° WT (Fig. 5B), also with a deeper minimum signal. These data supported the conformational differences suggested by FTIR. Some quantitative differences in WT spectra were observed between experiments, possibly from variations in batches of arachidonic acid or tau protein preparations. Qualitative differences between WT and MUT spectra were consistently observed within each experiment. To assure that the spectra observed were due to aggregates arising from the seeding reaction, and not simply those carried over from the 1° reaction, we serially diluted 1° WT and MUT reactions. The resulting spectra from the 4° dilutions are non-existent (Fig. 5C), thus aggregates in the 1° seeding reaction (which are diluted 1000x) are not sufficient to produce the signals observed in 4° reactions. We also ruled out the possibility that minor differences in protein concentration could account for the spectral differences between the samples (Fig. 5D).

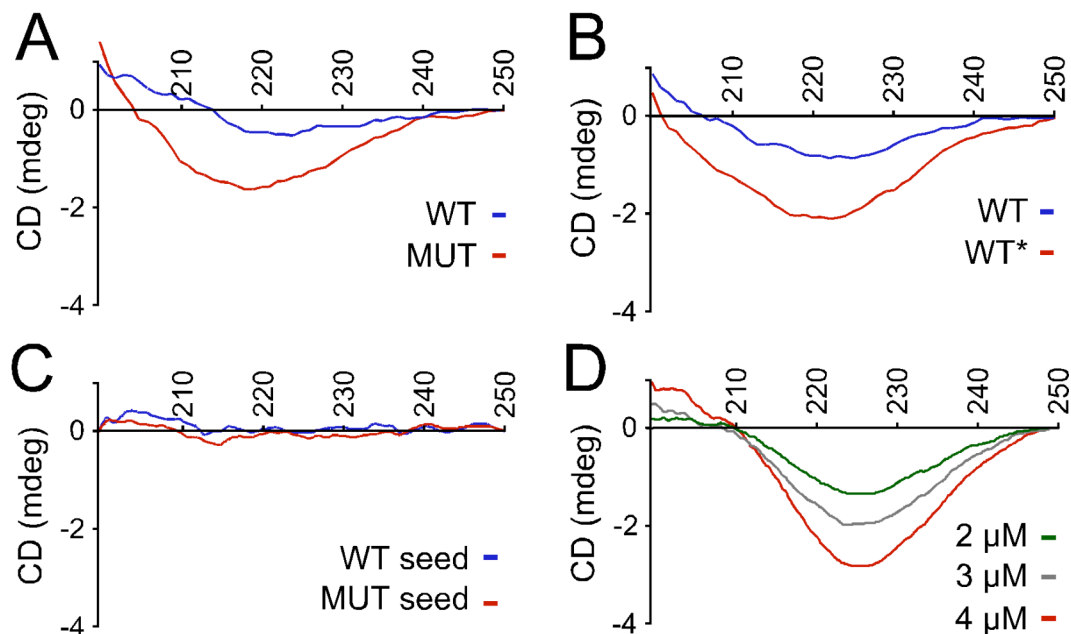


Figure 5: CD analysis of WT, MUT, and WT\* tau fibrils

- (A) Insoluble material from 1° WT and MUT fibrillization reactions have distinct CD spectra.
- (B) Insoluble material from 4° WT and WT\* fibrillization reactions have distinct CD spectra.
- (C) 1° WT and MUT seeds were used in three serial seeding reactions of buffer. 4° reactions were ultracentrifuged at 100,000 x g for 1 h, and pellets were resuspended in PBS. CD spectra are non-existent.
- (D) CD spectra of 4  $\mu$ M, 3  $\mu$ M, and 2  $\mu$ M, 1  $\mu$ M MUT fibrils. A 2  $\mu$ M decrease in concentration generates a 1 mdeg loss in CD spectrum intensity.

Spectra reflect four accumulations.



### **WT and WT\* fibrils have distinct fragilities**

Prior reports indicate that Sup35 prion strains are differentially susceptible to sonication-induced shearing (Tanaka et al. 2006), and long  $\beta$ 2-microglobulin amyloid fibrils exhibit deeper CD spectroscopic minima at 223 nm than short fibrils (Adachi et al. 2007), implying that CD changes before and after sonication can be used to evaluate fibril strength. Consequently, as an additional comparison of structural differences between the fibril types, we developed a method to evaluate the relative sensitivity of WT, MUT, and WT\* fibrils to sonication-induced breakage. First, we found that sonication treatment disproportionately disrupted 4° WT tau fibrils, but not MUT or WT\* fibrils based on AFM (Fig. 6A-C). In order to quantify fragility, we compared the CD spectra at 223 nm of the 1° reactions before and after sonication at 10% intensity. Like  $\beta$ 2-microglobulin fibrils, sonication of tau fibrils resulted in shorter fibrils that gave rise to a shallower minimum at 223 nm. After six experiments, the relative loss of MUT CD signal was 19% that of the loss in WT signal (Fig. 7A, C, D). MUT fibrils break down to an extent similar to WT fibrils after sonication at 20% intensity (data not shown). WT\* fibrils were also stronger than WT fibrils, and less disrupted by sonication. 4° WT\* fibrils exhibited 21% of the loss of signal vs. that of 4° WT fibrils (Fig. 7B, E, F). Thus, the differences between WT and WT\* observed by FTIR and CD spectroscopy are supported by distinct fibril fragilities.

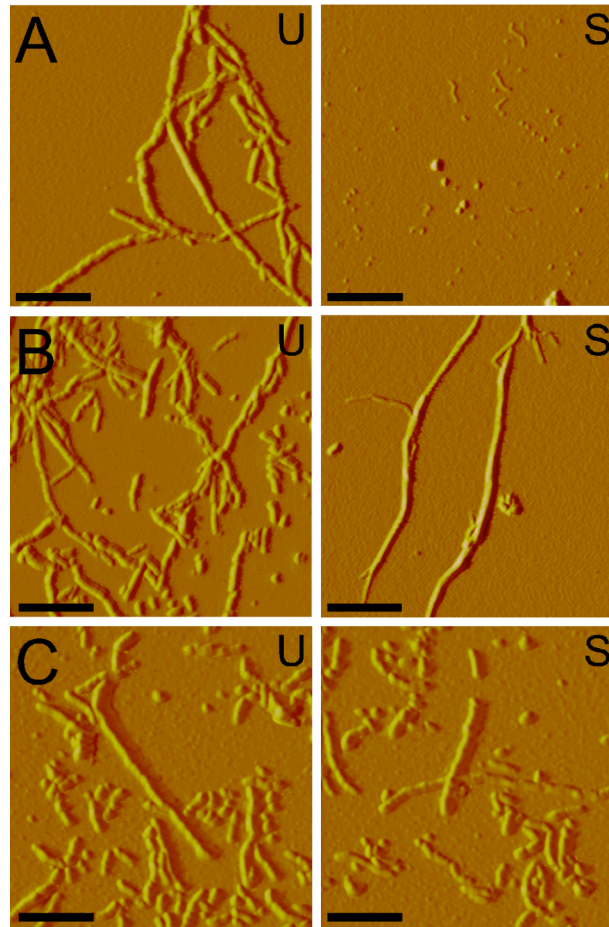


Figure 6: WT fibrils are more fragile than MUT and WT\* fibrils based on AFM

(A) 1° WT fibrils visualized by AFM, untreated (U), and after sonication (S).

(B) Identically prepared 1° MUT fibrils untreated (U), and after sonication (S) demonstrates the resistance of fibrils to sonication.

(C) 4° WT\* fibrils untreated (U), and after (S) sonication demonstrates the resistance of fibrils to sonication.

Scale bars = 0.25  $\mu\text{m}$ .

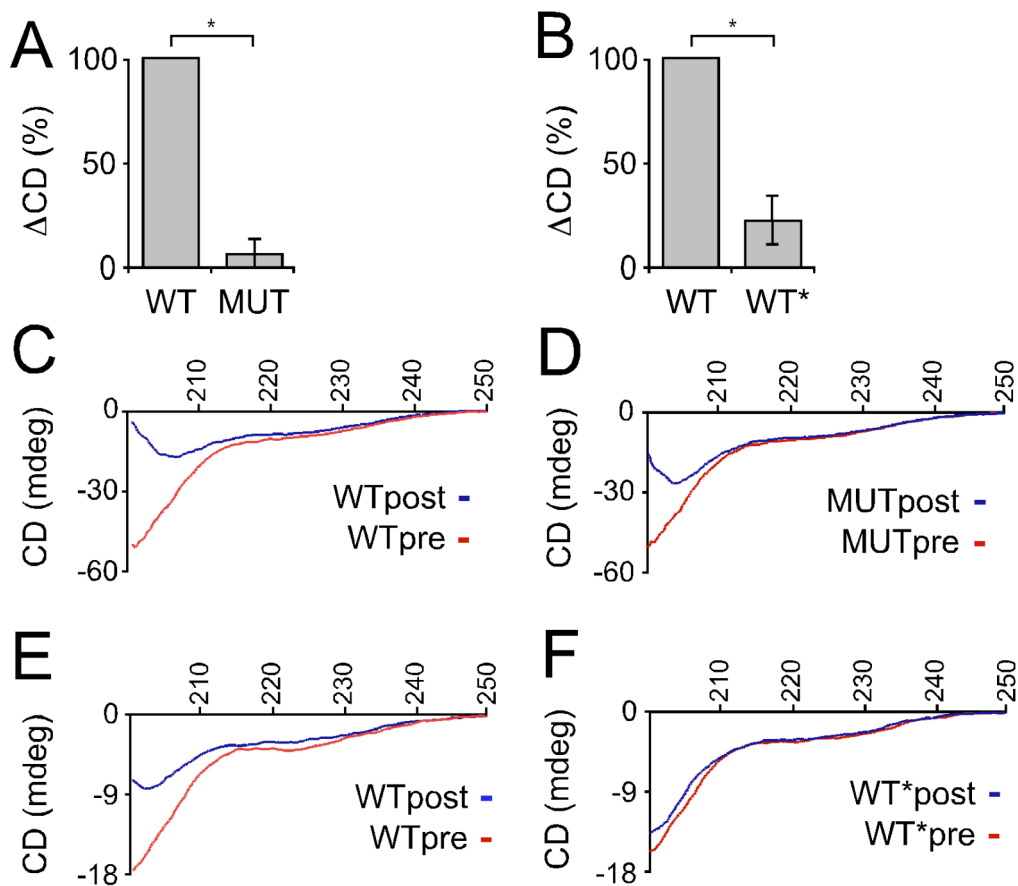


Figure 7: WT fibrils are more fragile than MUT and WT\* fibrils based on CD

- (A) Quantification of the loss of CD signal at 223 nm for WT and MUT 1° tau fibrillization reactions before and after sonication indicates MUT fibrils are stronger than WT fibrils.
- (B) Quantification of the loss of CD signal at 223 nm for WT and WT\* 4° tau fibrillization reactions before and after sonication indicates WT\* tau fibrils are stronger than WT fibrils.
- (C) 1° WT fibrillization reactions before (WTpre) and after (WTpost) sonication.
- (D) 1° MUT fibrillization reactions before (MUTpre) and after (MUTpost) sonication.
- (E) 4° WT fibrillization reactions before (WTpre) and after (WTpost) sonication.
- (F) 4° WT\* fibrillization reactions before (WT\*pre) and after (WT\*post) sonication.

Loss of signal for MUT and WT\* were calculated as a fraction of loss of signal for WT, which was set to 100%. \* $p=0.0156$ .  $n=6$ . Spectra reflect four accumulations.

### **WT and WT\* fibrils have different morphologies based on electron microscopy**

As a final comparison of the distinct structures, we used negative stain EM to evaluate the morphologies of the three fibril types. WT fibrils consisted of predominantly paired helical filaments (Fig. 8A, B), whereas MUT tau fibrils were more similar to straight filaments. They were thinner, lacked the typical paired helical morphology, and displayed a higher degree of flexibility (Fig. 8C, D). WT\* were distinct from WT in their lack of predominant paired helical structure, and had similar curvature and width to MUT tau (Fig. 8E, F). When three separate experiments were counted and quantified, we found significant differences in the proportion of paired helical filaments in WT fibril preparations versus MUT, and WT versus WT\*. 94% of WT fibrils appeared as paired helical filaments, while only 2.0% of MUT fibrils and 18% of WT\* fibrils were helical in nature, and instead appeared as straight, flexible fibrils (Fig. 8G). Taken together with the preceding experiments, these data confirm our findings that WT tau fibrils can adopt a distinct, stable, fibrillar structure that is propagated via templated conformation change.

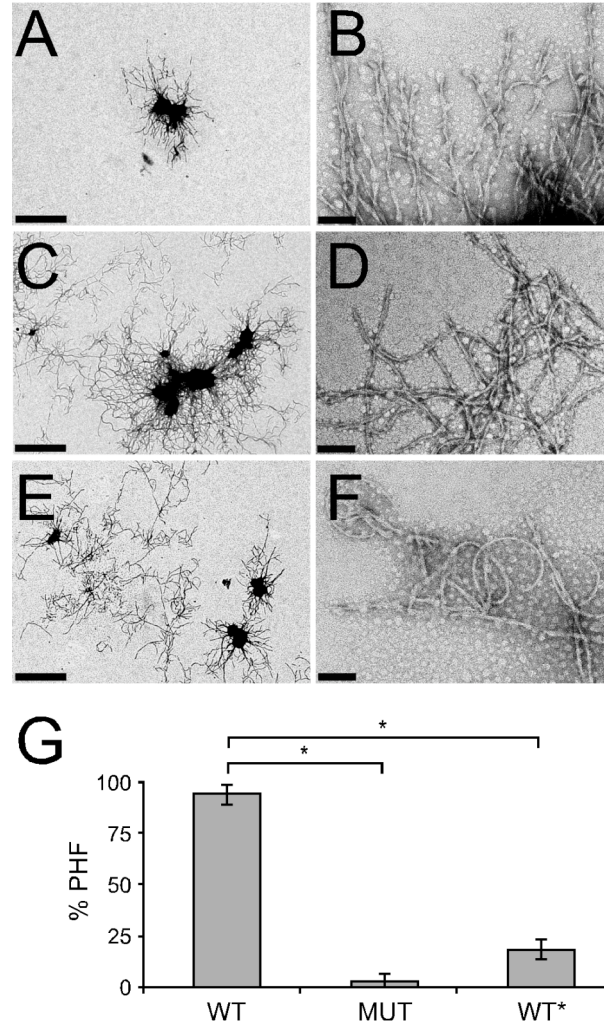


Figure 8: Negative stain electron microscopy of tau fibrils

- (A) Low, and (B) high magnification EM images show that 4° WT fibrils have a paired helical morphology.
- (C) Low, and (D) high magnification EM images show that 4° MUT fibrils have a distinct, curved morphology that lack the helical appearance of WT fibrils.
- (E) Low, and (F) high magnification EM images show that 4° WT\* fibrils have a curved morphology similar to MUT tau.
- (G) Quantification of three separate experiments. 94% of 4° WT fibrils are paired helical filaments (PHF), while 2.0% of MUT fibrils and 18% of WT\* fibrils are PHF.  $*=p<10^{-5}$ .

Scale bar in (A, C, E) = 1  $\mu$ m. Scale bar in (B, D, F) = 0.1  $\mu$ m.

## **Discussion**

In this study we tested the hypothesis that WT tau can assume distinct fibrillar conformations that are propagated serially by templated conformation change. We have exploited an artificial protein, MUT tau, containing two disease-causing mutations, as a convenient tool with which to drive WT tau into a distinct fibrillar conformation, termed WT\*. We have compared WT, MUT, and WT\* fibril conformations using four independent measures: FTIR spectroscopy, CD spectroscopy, sensitivity to sonication-induced breakage, and EM analysis of fibril morphology. Each of these assays demonstrates that WT\* represents a novel conformation of WT fibril that is maintained over time through templated conformation change.

Our data are consistent with the idea that sporadic tauopathies, which only involve WT tau, might derive phenotypic diversity from conformational differences in WT tau fibrils. In addition to MUT tau fibrils, we have also observed that  $\Delta$ K280 tau fibrils can seed a new conformation of WT tau (Fig. 9), suggesting that the ability to induce WT tau to adopt unique conformations by templated conformation change is not restricted to a particular seed. It remains to be determined to what extent a mutant tau protein in patients can trigger misfolding of the wild-type, and whether other factors might play a role. Indeed, the stimuli that induce WT tau to form fibrils of a unique conformation in sporadic tauopathy patients could be myriad: splice isoforms, post-translational modifications, a heterologous seed (e.g. A $\beta$ ), oxidation events, etc. Our experiments suggest a theoretical framework with which to consider phenotypic diversity in the

sporadic tauopathies: once WT tau is sent down a particular conformational path, whatever the inciting stimulus, it maintains this distinct conformation via templated conformation change.

Recent evidence from studies of prion disease suggests a strong link between the conformation of a fibrillar protein and the resultant phenotype (Tanaka et al. 2004; Legname et al. 2006). According to this model, once a protein adopts a particular fibrillar conformation, that conformation is propagated over time through subsequent seeded fibrillization reactions. The properties of a given fibril type (such as growth rate, fragility, and subsequent toxicity) play an important role in specifying phenotypic features (Tanaka et al. 2006). Our results support data reported by others that multiple amyloid-forming proteins have the ability to form distinct conformers based on templated conformation change (Petkova et al. 2005; Yamaguchi et al. 2005). Indeed, the seeding barrier that has been reported between P301L mutant tau and WT tau is reminiscent of prion strains (Miyasaka et al. 2001; Aoyagi et al. 2007), and is consistent with our hypothesis, which would allow for cross-seeding barriers to exist between tau mutants. Our studies indicate that, like other amyloid proteins such as A $\beta$ ,  $\beta$ 2-microglobulin, and prion protein, WT tau can adopt multiple distinct fibrillar conformations that are maintained over time via templated conformation change. In future experiments it will be fascinating to determine whether phenotypic diversity in sporadic tauopathies can be linked to unique WT tau fibril conformations.

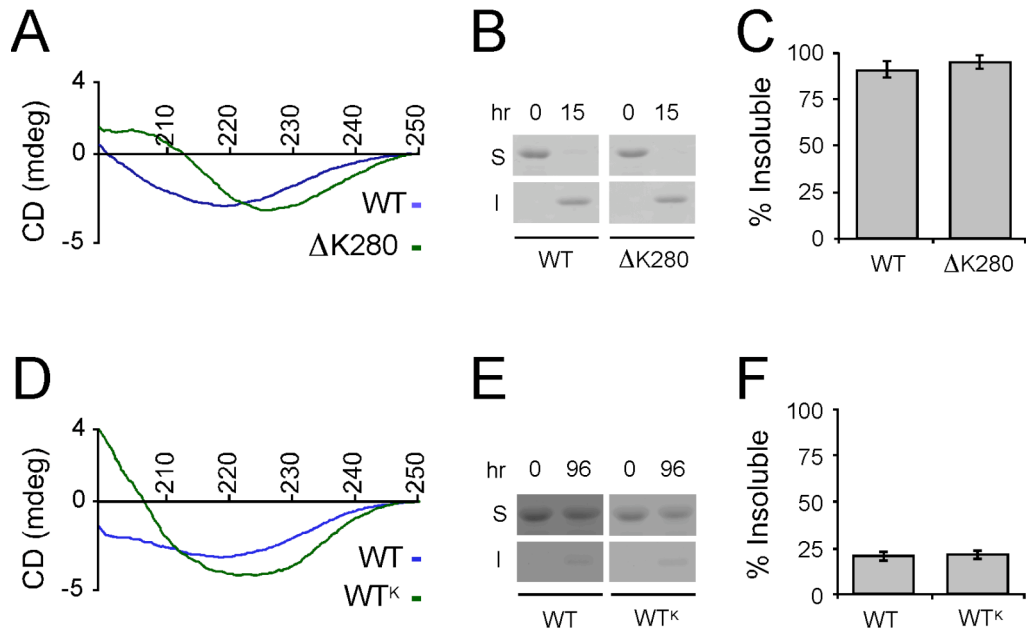


Figure 9:  $\Delta$ K280 seeds a novel conformation of WT fibril, WT<sup>K</sup>

- (A) The insoluble fraction of 1<sup>o</sup> WT and  $\Delta$ K280 reactions have distinct CD spectra.
- (B) After 15 h of fibrillization, most of the soluble tau monomer appears in the insoluble fraction after 100,000 x g ultracentrifugation and visualization via Coomassie stain.
- (C) Quantification of three separate experiments: after 15 h, 88% of WT tau monomer is insoluble, versus 94% of  $\Delta$ K280 tau.
- (D) The insoluble fraction of 4<sup>o</sup> WT and WT<sup>K</sup> reactions have distinct CD spectra.
- (E) After three serial seeding reactions and 96 h final growth, tau monomer appears in the soluble fraction after 100,000 x g ultracentrifugation and visualization via Coomassie stain.
- (F) Quantification of three separate experiments: after three serial seeding reactions ad 96 h final growth, 22% of WT and WT<sup>K</sup> tau is insoluble, indicating comparable degrees of fibrillization.

Spectra reflect four accumulations.



## **CHAPTER 3**

### **EXTRACELLULAR TO INTRACELLULAR PROPAGATION OF TAU**

#### **MISFOLDING**

## **Extracellular to Intracellular Propagation of Tau Misfolding**

Bess Frost<sup>1,3</sup>, Rachel L. Jacks<sup>1,3</sup>, and Marc I. Diamond<sup>1,2,3</sup>

From Departments of <sup>1</sup>Neurology, and <sup>2</sup>Cellular and Molecular Pharmacology, and  
<sup>3</sup>Biomedical Sciences Program

University of California, San Francisco

GH-S572B 600 16<sup>th</sup> Street

San Francisco, CA 94143-2280

Phone: 415-514-3646

Fax: 415-514-4112

Email: [marc.diamond@ucsf.edu](mailto:marc.diamond@ucsf.edu)

*[Reprinted from Journal of Biological Chemistry, March 16 2009]*

## Abstract

Tauopathies are neurodegenerative diseases characterized by aggregation of the microtubule-associated protein tau in neurons and glia. Although tau is normally considered an intracellular protein, tau aggregates are observed in the extracellular space, and tau peptide is readily detected in the cerebrospinal fluid of patients. Tau aggregation occurs in many diseases, including Alzheimer disease and frontotemporal dementia. Tau pathology begins in discrete, disease-specific regions, but eventually involves much larger areas of the brain. It is unknown how this propagation of tau misfolding occurs. We hypothesize that extracellular tau aggregates can transmit a misfolded state from the outside to the inside of a cell, similar to prions. Here we show that cultured cells take up extracellular tau aggregates, but not monomer. Internalized tau aggregates displace tubulin, co-localize with dextran, a marker of fluid-phase endocytosis, and induce fibrillization of intracellular full-length tau. These intracellular fibrils are competent to seed fibril formation of recombinant tau monomer *in vitro*. Finally, we observe that newly aggregated intracellular tau transfers between co-cultured cells. Our data indicate that tau aggregates can propagate a fibrillar, misfolded state from the outside to the inside of a cell. This may have important implications for understanding how protein misfolding spreads through the brains of tauopathy patients, and is potentially relevant to myriad neurodegenerative diseases associated with protein misfolding.

## **Introduction**

Tau filament deposition in Alzheimer disease (AD), frontotemporal dementia (FTD), and other tauopathies correlates closely with cognitive dysfunction and cell death (Lee et al. 2001). Mutations in the tau gene cause autosomal dominant tauopathy, implicating tau as the proximal cause (Hutton et al. 1998; Poorkaj et al. 1998; Spillantini, Murrell et al. 1998). Specific disease phenotypes are defined by the early sites of pathology. For example, AD is characterized by memory loss that derives from involvement of hippocampal neurons, whereas FTD is characterized by personality changes that result from frontal lobe involvement (Liu et al. 2004). Pathology ultimately spreads to involve much larger regions of brain. Studies on AD patients show a progressive, stereotyped spread of tau deposits from the transentorhinal cortex to the hippocampus, and eventually to most cortical areas (Braak et al. 1991; Braak et al. 1997; Delacourte et al. 1999). Others have correlated the distribution of neurofibrillary tangles of tau in AD brains with trans-synaptic distance from the affected areas (Arnold et al. 1991). A similar spread affecting different subsets of neurons has been observed in other sporadic tauopathies, such as progressive supranuclear palsy (Delacourte 2005). It is unknown why tau misfolding progresses through the brain—whether it is a sequence of cell autonomous processes, or whether a toxic factor is involved. Loss of synaptic connections and cell death may expose healthy cells to toxic factors and decrease available neurotrophins (Akiyama et al. 2000; Delacourte 2005). Another possibility is that the tau protein itself serves as the agent of trans-cellular propagation. For example, it has been shown that extracellular tau is toxic to cultured neuronal cells (Gomez-Ramos et al. 2006; Gomez-

Ramos et al. 2008). This is consistent with the observation that immunotherapy against tau reduces pathology in a mouse model (Asuni et al. 2007).

Tau is well known as an intracellular protein that stabilizes microtubule filaments (Weingarten et al. 1975), however, it is readily detected in cerebrospinal fluid (Vandermeeren et al. 1993), and as extracellular aggregates, termed “ghost tangles,” in diseased brain. These are comprised predominantly of the microtubule-binding region (MTBR), the functional and pathogenic core of the tau protein (Endoh et al. 1993). We hypothesize that tau aggregates present in the extracellular space enter naive cells and induce misfolding of intracellular tau. We have tested this idea using cellular studies, biochemistry, and atomic force microscopy (AFM).

## Experimental Procedures

***Tau Expression, Purification, and Fibrillization.*** The MTBR (amino acids 243 to 375) of full-length (P10636-8) wild-type tau was subcloned into pRK172. HA-tagged MTBR tau contains the sequence YPYDVPDYA on its C-terminus. Recombinant tau MTBR was prepared as described previously from Rosetta (DE3)pLacI competent cells (Novagen), exploiting the heat stability of tau protein followed by cation exchange chromatography (Goedert et al. 1990). Single-use aliquots were stored at -80 °C in 10 mM HEPES and 100 mM NaCl (pH 7.4). To induce fibrillization of tau monomer, the MTBR was incubated at room temperature without agitation in 5 mM DTT, 10 mM HEPES (pH 7.4), 100 mM NaCl, and 150  $\mu$ M arachidonic acid (Sigma-Aldrich). Incubation times from 3 h to 24 h had similar cellular interactions.

***Atomic Force Microscopy and Antibody Decoration.*** Tau fibrillization reactions were incubated on freshly cleaved mica (Ted Pella, Inc.) for 2 min. The sample was then rinsed twice with 200  $\mu$ l of water. After washing, samples exposed to antibody decoration were incubated with 20  $\mu$ g/ml Tau5 antibody (BD Biosciences) for 2 min. The sample was rinsed twice with water and left to dry for at least 1 h prior to tapping mode atomic force microscopy (Digital Instruments).

***Western Blots.*** HEK293 or C17.2 cells were seeded 300,000 or 75,000 cells/well, respectively, in a 24-well plate. The following day, cells were transfected with 1.2  $\mu$ g full-length wild-type tau-YFP or MTBR-YFP using Lipofectamine2000 (Invitrogen)

according to the manufacturer's recommendations. After 15 h, cells were replated 1:4 in a 24-well plate, allowed to readhere for 5 h, and treated with 0.4  $\mu$ M tau buffer, monomer, or aggregates. After 15 h, cells were harvested with 0.25% trypsin for 3 min, pelleted, and lysed in 40  $\mu$ l of 1.0% Triton in PBS plus a protease inhibitor tablet (Roche) (lysis buffer). As an additional control, untreated cells were treated with an equivalent concentration of aggregates after lysis. Soluble and insoluble fractions of cell lysates were obtained by centrifugation of lysates at 14,000 rpm for 10 min at 4 °C. Insoluble pellets were washed twice with lysis buffer and resuspended in 40  $\mu$ l of lysis buffer. For whole cell lysates, cells were harvested and syringe lysed in PBS plus a protease inhibitor tablet. Triton soluble and insoluble fractions were resolved by SDS-PAGE on a 7.5% gel, while whole cell lysates were resolved by SDS-PAGE on a 4-15% gradient gel (BioRad). Following transfer to a nylon membrane (Millipore), blots were probed with either the Tau5 antibody (1:5,000, BD Biosciences), which recognizes an epitope in the polyproline region of tau protein (intracellular transfected tau) that is not present in the MTBR (extracellular tau), or the GFP sc-8334 antibody (1:2,000, Santa Cruz Biotechnology). Blots were stripped and reprobed with the I-19-R anti-actin antibody (1:2,000, Santa Cruz Biotechnology). HA Y.11 (1:2,000, Covance) was used to probe for MTBR-HA tau.

***Immunofluorescence.*** All cells were grown on poly-ornithine coated glass coverslips for microscopy. For visualization of intracellular tau-YFP and MTBR-YFP, cells were transfected with tau-YFP or MTBR-YFP. Cells were fixed with -20 °C methanol for 7 min and stained for  $\alpha$ -tubulin (1:500; Sigma-Aldrich) followed by secondary staining

with a rhodamine conjugated anti-mouse antibody A546 (1:500; Molecular Probes). To visualize MTBR-AF488 aggregates inside cells, buffer, MTBR monomer, and MTBR aggregates were labeled with 62.5 ng/ $\mu$ l AF488 (Molecular Probes) for 1 h at room temperature and then overnight at 4 °C. Reactions were quenched with 100 mM glycine and added to cells. After 15 h, cells were treated with either PBS or 0.25% trypsin for 3 min, and allowed to recover for 5 h before methanol fixation and staining for  $\alpha$ -tubulin. Z-stacks were rendered into a 3-D image using the NIS-Elements AR 3.0 software (Nikon) from which an apical to distal slice containing the aggregate was obtained. For co-labeling with dextran, C17.2 cells were treated with MTBR-AF488 and 50  $\mu$ g/ml rhodamine-dextran (10,000 MW, pH neutral, Molecular Probes) for 4 h. Cells were trypsinized, fixed with 4.0% PFA, and prepared as described above. For extracellular MTBR-HA and intracellular tau-YFP co-localization studies, C17.2 cells expressing tau-YFP were incubated with buffer, MTBR-HA monomer, or MTBR-HA aggregates for 15 h. Cells were trypsinized and allowed to recover as described before fixation with 4.0% PFA. Cells were stained with the HA-Y11 antibody (1:1,000, Santa Cruz Biotechnology), followed by secondary labeling with rhodamine conjugated anti-rabbit antibody (1:500; Molecular Probes). For co-culture experiments, C17.2 cells were transfected separately with MTBR-YFP and SV40-mCherry or tau-YFP and mCherry. Cells were treated with tau buffer, 0.4  $\mu$ M tau monomer, or MTBR tau aggregates. After the indicated co-culture incubation, cells were fixed for 7 min with 4.0% PFA, stained with DAPI (Sigma-Aldrich), and mounted on glass slides for imaging. Confocal microscopy was performed on a C1sl confocal microscope (Nikon Instruments Inc.).



**Flow Cytometry.** AF488 containing buffer or MTBR-AF488 were incubated with cells for the time indicated. Cells were harvested with 0.25% trypsin for 3 min and resuspended in PBS plus 10% FBS prior to flow cytometry. Cells were counted in a FACSCalibur (BD Biosciences) flow cytometer. Each experiment was repeated four times, and 10,000 cells were counted in each individual experiment. For co-culture experiments, MTBR-YFP or tau-YFP expressing cells were co-cultured with SV40-mCherry-expressing cells. Tau-YFP expressing cells were treated with buffer, MTBR monomer, or MTBR aggregates for indicated durations prior to flow cytometry. In order to collect dual positive cells, cells were sorted in a FACSARIA cell sorter (BD Biosciences).

**Sarkosyl Extraction.** 1.0% Sarkosyl-insoluble material was purified from cell lysates from a confluent 5 cm cell culture dish as described previously (Greenberg et al. 1990), with some modifications. Cell lysis buffer consisted of 10 mM Tris-HCl (pH 7.4), .8 M NaCl, 1 mM EGTA, 5 mM EDTA, 10% sucrose, and a protease inhibitor tablet (Roche). Sarkosyl-insoluble pellets were resuspended in 50  $\mu$ l of 10 mM HEPES and 100 mM NaCl (pH 7.4). When Sarkosyl-insoluble material from cells was used to seed tau monomer, the reactions contained 90  $\mu$ l of 4.0  $\mu$ M MTBR tau monomer, 5 mM DTT, 100 mM NaCl, 10 mM HEPES, and 10  $\mu$ l of syringe-sheared Sarkosyl-insoluble material from a 5 cm dish of buffer or MTBR aggregate treated, tau-YFP expressing cells.

## Results

### **Full-length tau does not aggregate spontaneously in cells; truncated tau forms inclusions**

To characterize the cellular activities of tau, we used four different constructs (Fig. 1). For expression in mammalian cells, we fused either full-length tau (441 amino acids), or the microtubule-binding region (amino acids 243-375) to yellow fluorescent protein (YFP); (tau-YFP and MTBR-YFP). For *in vitro* tau fibrillization reactions, we created MTBR tau with a hemagglutinin tag (MTBR-HA) and untagged MTBR. We expressed tau-YFP in C17.2 neuronal precursor cells (Ryder et al. 1990) by transient transfection. Tau-YFP co-localized with microtubules (Fig. 2A), as others have reported (Trinczek et al. 1995; King et al. 2006), and did not readily form inclusions (Fig. 2D). In contrast, MTBR-YFP did not bind microtubules, and readily formed inclusions (Fig. 2B, D) when expressed at a level comparable to tau-YFP (Fig. 2C).



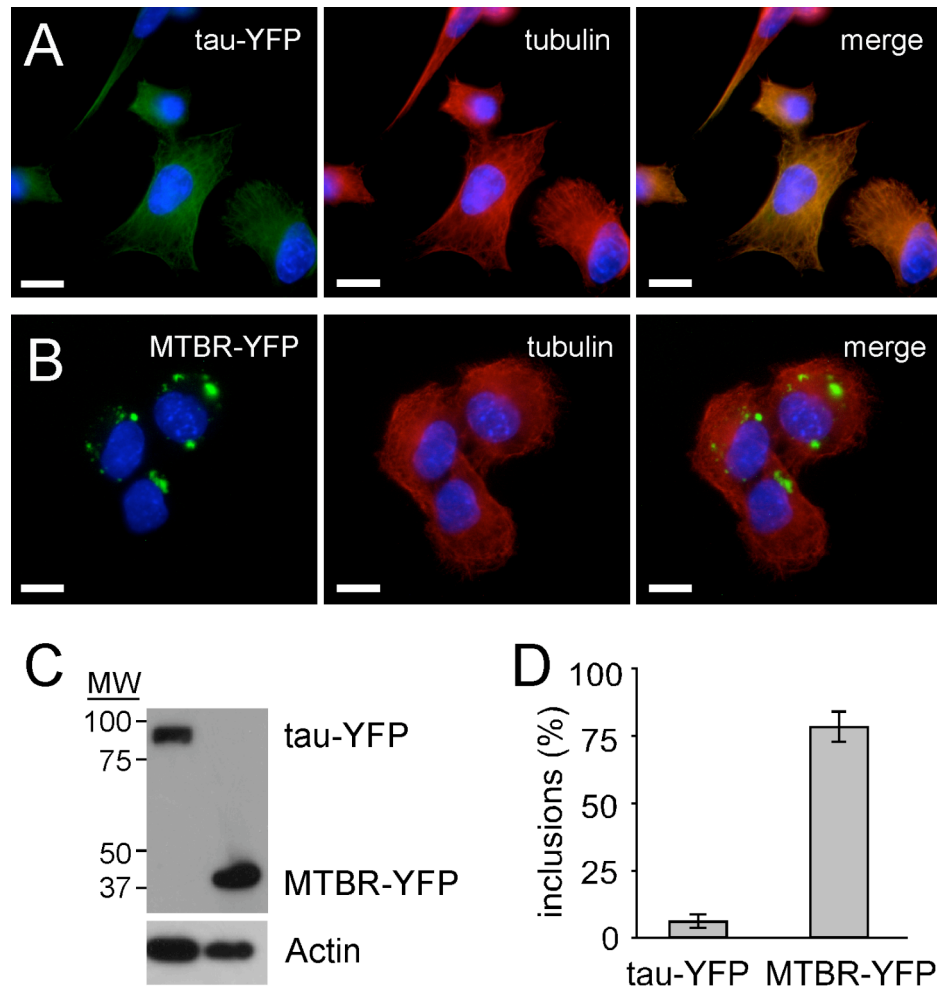


Figure 2: Full-length tau-YFP binds microtubules while MTBR-YFP aggregates in C17.2 neural cells

- (A) Tau-YFP co-localizes with tubulin when transfected into C17.2 cells.
- (B) MTBR-YFP does not co-localize with tubulin and spontaneously aggregates when transfected into C17.2 cells.
- (C) Western blot showing similar expression levels of tau-YFP and MTBR-YFP. Blots were probed with GFP and actin antibodies.
- (D) Based on counting transfected cells, 6.0% of cells have spontaneous aggregation of tau-YFP, while 79% of cells have spontaneous aggregation of MTBR-YFP (n=4, 100 transfected cells counted per experiment).

### **Tau aggregates enter C17.2 cells**

It has been shown previously that aggregated amyloid proteins A $\beta$ , PrP, and expanded polyglutamine can gain entry into cells (Kanu et al. 2002; Yang et al. 2002; Magalhaes et al. 2005; Ren et al. 2009). Thus, we tested for uptake of recombinant tau aggregates into C17.2 cells. First, we prepared recombinant MTBR-HA, and used arachidonic acid to stimulate its fibrillization, which we detected using AFM (Fig. 3A). We found that these aggregates were completely digested when treated with 0.125% trypsin for 1 min (Fig. 3B). This is 50% of the level of trypsin used to re-plate cells in tissue culture (which are treated with 0.25% trypsin for 3 min), indicating relative sensitivity of the extracellular aggregates to proteolysis.

To determine if tau aggregates were taken into cells, we labeled MTBR tau monomer and aggregates with AlexaFluor488 (AF488). We exposed C17.2 cells to AF488-containing buffer, AF488 conjugated to MTBR monomer, or MTBR aggregates. After 3 and 9 h, we harvested the cells from the plates by treating cells with 0.25% trypsin for 3 min. We quantified AF488 fluorescence using flow cytometry (Fig. 4A). Fluorescence signal due to background uptake of unconjugated AF488 in the buffer was subtracted from all samples. We observed significantly more uptake of aggregates compared to monomer at both time points (Fig. 4A). Direct visualization of these cells before and after trypsinization confirmed the conclusions derived from the flow cytometry experiment, indicating internalization of the aggregated species by the cells (Fig. 4B). Aggregates of extracellular-derived tau of various sizes were observed in cultured cells.

To verify that the tau present after trypsinization was indeed intracellular, we stained MTBR-AF488 aggregate-treated cells for tubulin, and visualized the cells using confocal microscopy. In cells that were treated with aggregates and imaged before trypsinization, both intracellular and extracellular membrane-associated aggregates were observed (data not shown). In trypsin-treated cells, however, the internalized aggregates displaced tubulin (Fig. 4C), and were present in the same plane as tubulin (bar, Fig. 4C), confirming their intracellular locale.

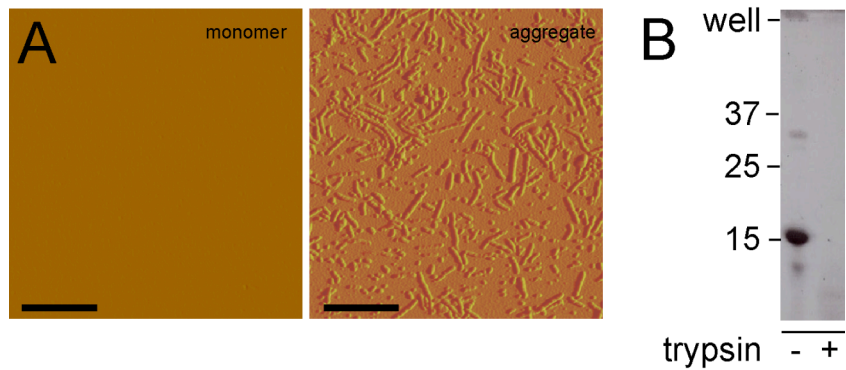


Figure 3: Tau aggregates are sensitive to trypsin

- (A) Recombinant MTBR tau was prepared *in vitro* and induced to fibrillize using arachidonic acid. Tau monomer is not detectable via AFM. After 24 h of incubation with arachidonic acid, however, tau is highly aggregated, forming many oligomeric and fibrillar species. Scale bars = 600 nm.
- (B) Aggregated tau was treated with buffer or 0.125% trypsin for 1 min and resolved by SDS-PAGE 4-15% gradient gel followed by Coomassie stain. Aggregated tau is very sensitive to trypsin digestion.

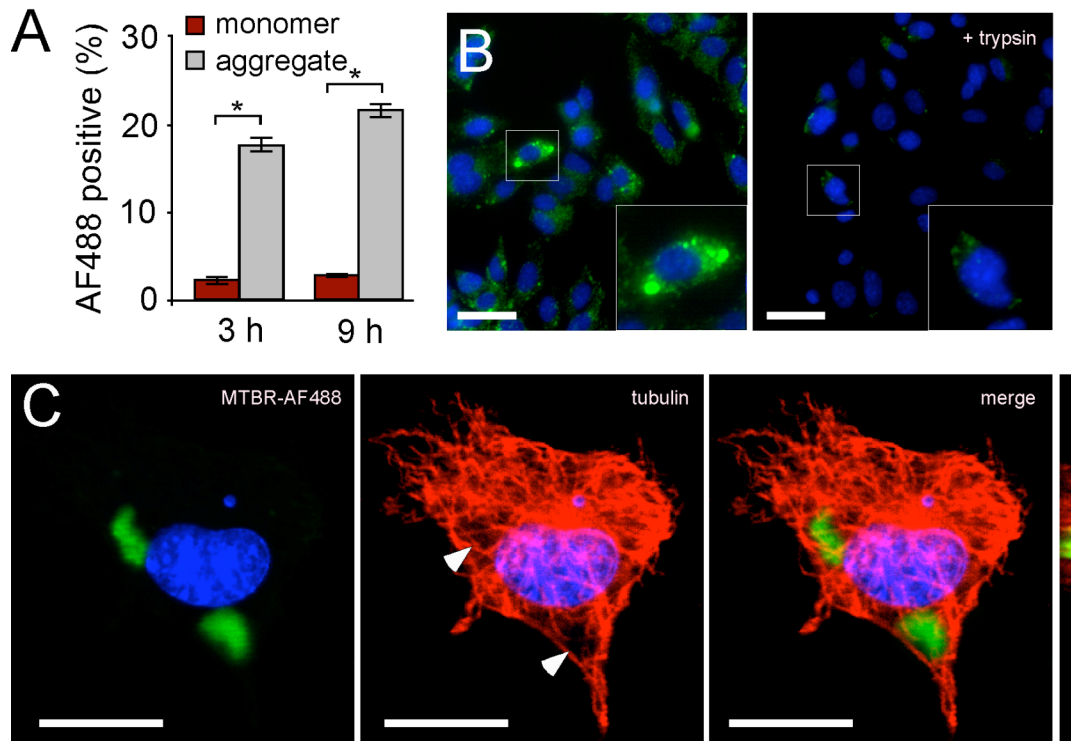


Figure 4: C17.2 cells take up aggregated tau

- (A) C17.2 cells were exposed to AF488 containing buffer, AF488-labeled monomer, or aggregates. After 3 h and 9 h, cells were harvested by 0.25% trypsin treatment. Intracellular AF488 fluorescence was quantified by flow cytometry. After 3 h, 2.0% of monomer treated cells scored positive, versus 18% for aggregate treated cells. After 9 h, 3.0% of monomer treated cells scored positive, versus 22% for aggregate treated cells.  $*p < 10^{-6}$  (unpaired t-test  $n=4$ , 10,000 cells counted per experiment).
- (B) MTBR-AF488 aggregate treated C17.2 cells with or without trypsin treatment visualized by confocal microscopy. Scale bar = 30  $\mu\text{m}$ .
- (C) MTBR-AF488 aggregated treated C17.2 cells stained for tubulin visualized via confocal microscopy after treatment with 0.25% trypsin illustrates internalized aggregates. Arrows indicate displacement of tubulin. An apical-to-distal slice (bar obtained from a 3-dimensional image rendered from z-stacks shows MTBR-AF488 in the same plane as tubulin. Scale bar = 10  $\mu\text{m}$ .



### **Tau aggregates enter C17.2 cells and co-localize with dextran**

It has been shown previously that exogenously-derived A $\beta$  and PrP aggregates co-localize with dextran, a marker of fluid-phase endocytosis. Such aggregates do not co-localize with cholera toxin subunit B, a marker of lipid rafts (Magalhaes et al. 2005). We exposed C17.2 cells to MTBR-AF488 tau aggregates and dextran. 24% of tau aggregates co-localized with dextran (n=3, 200 aggregates counted per experiment) (Fig. 5), but did not co-localize with cholera toxin B (data not shown). This suggests that tau aggregates enter cells via an endocytic pathway involving engulfment by the cell membrane, rather than the simple penetration of the membrane, as has been proposed previously for other amyloid forming proteins (Kayed et al. 2004).

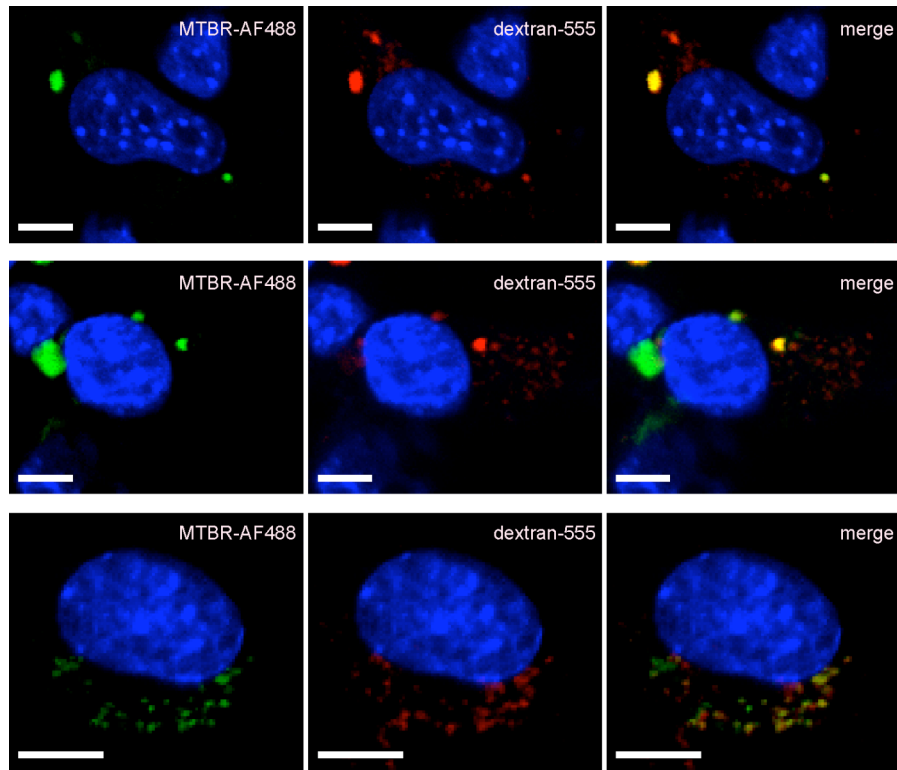


Figure 5: Extracellularly-derived aggregates co-localize with a marker of endocytosis

Multiple images of C17.2 cells treated with MTBR-AF488 aggregates and rhodamine-dextran exhibit co-localizing and non-co-localizing aggregates. Scale bars = 5  $\mu$ m.

### **Exogenous tau aggregates induce aggregation of intracellular full-length tau-YFP**

Tau fibrils propagate *in vitro* via seeded polymerization (Friedhoff et al. 1998). We thus tested whether extracellular tau aggregates that enter cells would trigger the misfolding of intracellular tau-YFP. We transiently transfected HEK293 cells with tau-YFP. We treated these cells with buffer, MTBR monomer, or MTBR aggregates. After 15 h, cells were harvested, lysed in 1.0% Triton, and extracts were fractionated by centrifugation at 15,000 x g. After SDS-PAGE, western blot was performed using the Tau5 antibody, which recognizes a motif in the polyproline region of full-length tau that is not present in the MTBR. Cells treated with aggregates, but not buffer or monomer, contained detergent-insoluble tau-YFP (Fig. 6A). We repeated this experiment in C17.2 cells, including a negative control in which we mixed MTBR aggregates with cell lysate containing tau-YFP prior to rule out induction of aggregation following lysis (Fig. 6B). To confirm tau-YFP aggregation in C17.2 cells, detergent-free whole cell lysates were created and resolved by western blot with the Tau5 antibody. We observed tau-YFP aggregates at the top of the well when cells were treated with MTBR aggregates, but not after treatment with buffer or monomer (Fig. 6C). To determine the specificity of aggregate induction, we treated tau-YFP expressing cells with aggregates of huntingtin exon 1 containing 53 glutamines. Exogenous aggregated huntingtin had no effect on intracellular tau-YFP aggregation based on western blot (data not shown).

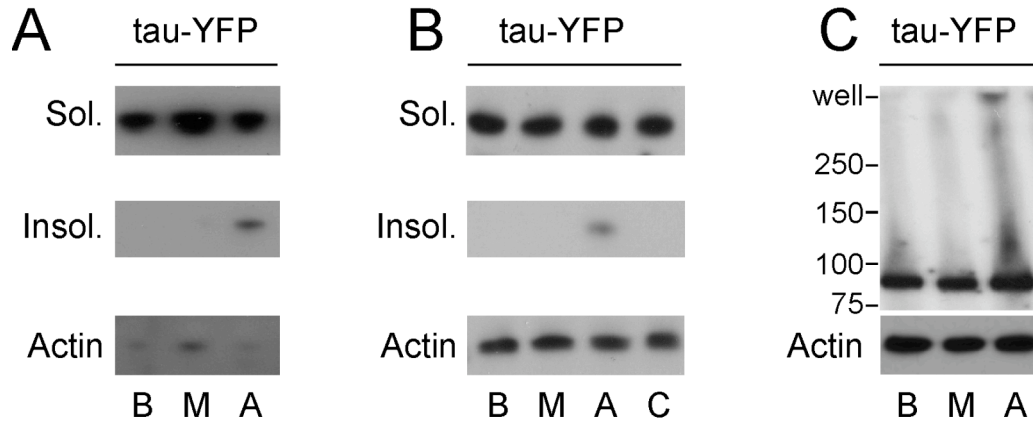


Figure 6: Extracellular tau enters cells and induces aggregation of full-length tau-YFP in HEK293 and C17.2 cells

- (A) HEK293 cells or (B) C17.2 cells expressing tau-YFP were treated for 15 h with buffer, B, monomer, M, or MTBR aggregates, A, followed by 1.0% Triton detergent fractionation. Control cells, C, were lysed and treated with aggregates. Soluble and insoluble tau-YFP bands were detected using the Tau5 antibody, with actin as a loading control. Treatment with tau aggregates increased insoluble tau-YFP in both cell types.
- (C) C17.2 cells expressing tau-YFP were treated for 15 h with buffer, MTBR monomer, or MTBR aggregates, followed by syringe lysis in PBS. The whole cell lysate was loaded onto a 4-15% SDS-PAGE gel, and blotted with a GFP antibody or an actin antibody to control for loading. Full-length aggregated tau-YFP appears in the well when cells are treated with MTBR aggregates.

### **Intracellular aggregated MTBR-YFP and tau-YFP transfer between co-cultured cells**

Taken together, these experiments indicated that extracellular tau aggregates enter cells and induce misfolding of intracellular tau, but left uncertain whether this was due to a direct association of exogenous and endogenous protein. Thus, we used double-label fluorescence confocal microscopy to test for co-localization of exogenous MTBR-HA and endogenous tau-YFP. After treatment with MTBR-HA aggregates for 15 h and visualization via confocal microscopy, we observed intracellular inclusions consisting of both exogenously and endogenously derived protein (Fig. 7A), most of which co-localized. 74% of aggregates observed were composed of both MTBR-HA and tau-YFP; 23% of aggregates were composed only of tau-YFP; and 3.0% of aggregates were composed only of MTBR-HA (Fig. 7B). Tau-YFP aggregates observed in the absence of MTBR-HA co-localization may arise from self-seeding, or may contain MTBR-HA seeds that are too small to detect via immunofluorescence.

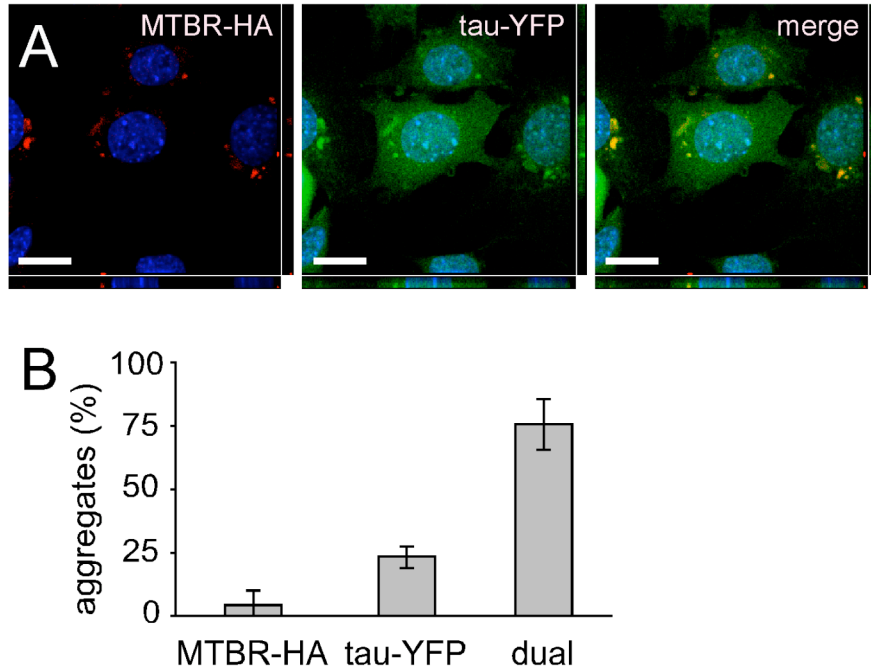


Figure 7: Extracellular tau enters cells and co-localizes with induced full-length tau-YFP aggregates in C17.2 cells

- (A) C17.2 cells expressing tau-YFP were exposed to MTBR-HA aggregates, and double label confocal microscopy was performed using an HA antibody (red channel) and direct visualization of YFP (green channel). A representative example of co-localization between MTBR-HA (exogenous) and tau YFP (endogenous) aggregates is shown. Scale bar = 10  $\mu$ m.
- (B) 3.0% of aggregates were composed of MTBR-HA in the absence of tau-YFP aggregates; 23% of aggregates were composed of tau-YFP in the absence of MTBR-HA aggregates; 74% of aggregates were dual fluorescent, composed of tau-YFP and MTBR-HA (n=3, 100 aggregates counted per experiment).

### **Extracellular tau aggregates induce fibrillization of intracellular tau-YFP**

To rule out the possibility that exogenously-derived aggregated tau caused disordered aggregation of intracellular tau-YFP, rather than fibrillization, we purified induced tau-YFP aggregates from cells. We treated C17.2 cells expressing tau-YFP with buffer or aggregates, and examined the Sarkosyl-insoluble fraction (Greenberg et al. 1990) from cell lysates using AFM. No fibrillar material was observed except in cells exposed to exogenous MTBR tau aggregates (Fig. 8A). To confirm that these fibrils were derived from intracellular full-length tau-YFP, and not the exogenous MTBR tau aggregates or other proteins, we used antibody decoration (DePace et al. 2002) with the Tau5 antibody. We observed an increase in fibril diameter along the length of the fibrils in Tau5 treated extracts, indicating the purified fibrils were composed of tau-YFP (Fig. 8B). We next used Sarkosyl-insoluble tau-YFP purified from C17.2 cells to seed the fibrillization of recombinant MTBR *in vitro*, confirming the conversion of tau-YFP to a fibrillar form that is competent to seed aggregation of tau monomer (Fig. 8C). Antibody decoration of the seeded fibrils using the Tau5 antibody produced isolated densities on the fibrils, confirming the source of the seed as tau-YFP (Fig. 8D). Thus, exposure to exogenous tau aggregates induces intracellular tau-YFP to form fibrils that are competent to seed further aggregation.

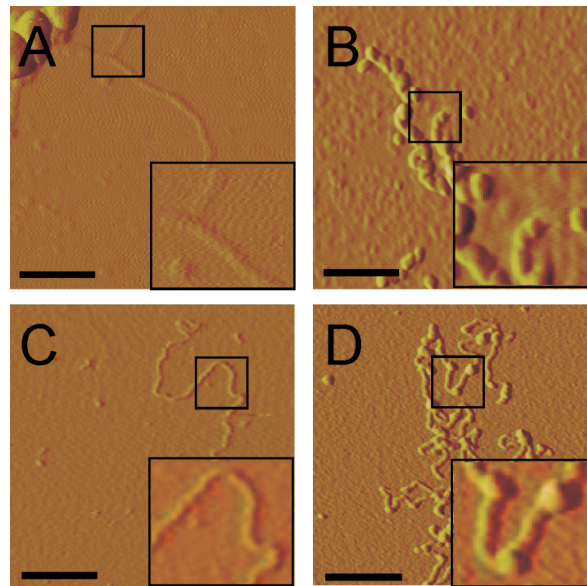


Figure 8: Induced tau-YFP aggregates in C17.2 cells are fibrillar and seed MTBR fibrillization *in vitro*

C17.2 cells, in which tau-YFP aggregation was induced by treatment with MTBR aggregates, were extracted with Sarkosyl.

- (A) Insoluble material was visualized by AFM, which demonstrates fibrils.
- (B) Tau5 antibody labeling increases the diameter of the observed fibrils, indicating their principle constituent is tau-YFP.
- (C) Sarkosyl extracted tau-YFP fibrils from aggregate-treated cells were used to seed the fibrillization of recombinant MTBR *in vitro*. The resultant fibrils were visualized by AFM.
- (D) MTBR fibrils seeded by tau-YFP were exposed to Tau5 antibody, which labels the tau-YFP seeds within the MTBR fibrils.

Scale bars = 0.2  $\mu\text{m}$ .



### **Intracellular tau-YFP aggregates transfer between co-cultured cells**

We next tested whether intracellular tau aggregates transfer between co-cultured cells. We separately transfected cells with either MTBR-YFP or mCherry (a red fluorescent protein variant), and then co-cultured them for 24 h. As a control, we cultured MTBR-YFP and mCherry cells separately, and mixed them immediately prior to flow cytometry. Co-cultured cells had significantly more YFP/mCherry dual positive cells (Fig. 9A). Based on four independent experiments, 0.48% of mixed cells (i.e. background) scored as dual-fluorescent, versus 1.6% of co-cultured cells (Fig. 9B). Dual positive cells were collected and viewed via fluorescence microscopy. This confirmed the presence of MTBR-YFP inclusions inside cells expressing mCherry (Fig. 9C), indicating that transfer of MTBR-YFP aggregates had occurred. To determine if the transfer of tau aggregates between co-cultured cells is inducible, we co-cultured cells expressing full-length tau-YFP and mCherry and initiated misfolding of tau-YFP by exposing cells to MTBR tau aggregates for 48 h (Fig. 10A). Treatment with aggregated species caused tau-YFP aggregation, and transfer of these species to 1.0% of the mCherry cells (Fig. 10B). We sorted dual positive cells, and imaged them with fluorescence microscopy. This confirmed the presence of tau-YFP inclusions in mCherry-expressing cells (Fig. 10C). Simple cell fusion was unlikely to have occurred at a significant rate, since buffer and monomer treated cells did not score positive. Thus, spontaneously formed MTBR-YFP tau intracellular inclusions or induced full-length tau-YFP inclusions spontaneously transfer between co-cultured cells.

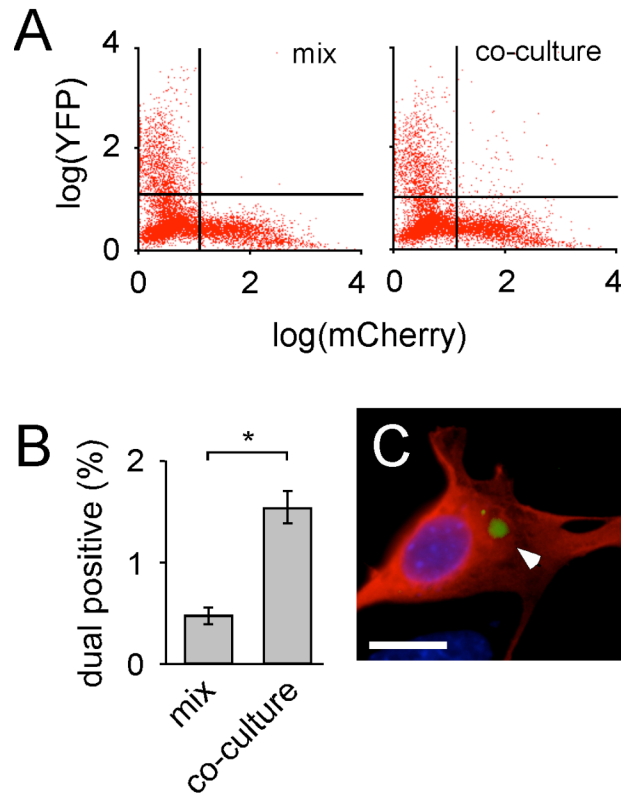


Figure 9: MTBR-YFP aggregates transfer between co-cultured cells

- (A) Cells were transfected separately with mCherry or MTBR-YFP. The two cell populations were either mixed immediately prior to analysis, or co-cultured for 24 h. Flow cytometry was used to quantify dual positive cells. (10,000 cells sorted per condition).
- (B) Quantification of flow cytometry revealed that 0.5% of cells scored positive for mCherry and YFP (upper right quadrant of cell plot) when cells were simply mixed prior to sorting, versus 1.5% of cells that scored dual-positive when cells were co-cultured for 24 h, indicating transfer of MTBR-YFP between cells.  $*p < 10^{-5}$  (unpaired t-test,  $n=4$ , 10,000 cells sorted per condition).
- (C) Dual positive cells were collected via FACS, fixed and mounted. A MTBR-YFP inclusion (white arrow) is visible within an mCherry-expressing cell. Scale bar = 10  $\mu\text{m}$ .

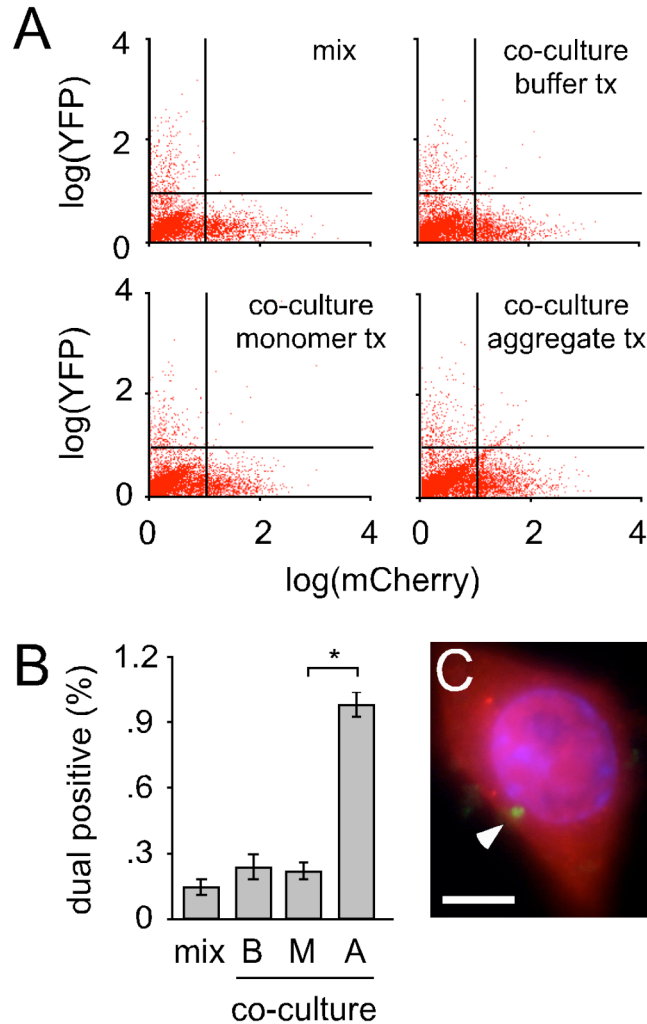


Figure 10: Tau-YFP aggregates transfer between co-cultured cells

- (A) Cells were transfected separately with mCherry or tau-YFP. The two cell populations were either mixed immediately prior to analysis, or co-cultured for 48 h. Co-cultured cells were treated with buffer, monomer, or aggregates, followed by flow cytometry. (10,000 cells sorted per condition).
- (B) Quantification of flow cytometry revealed that 0.15% of cells scored positive for mCherry and YFP (upper right quadrant of cell plot) when cells were simply mixed prior to sorting. 0.3% and 0.25% of cells are dual-positive when cells are treated with buffer or monomer, versus 1.0% when treated with tau aggregates, indicating transfer of aggregated full-length tau YFP between cells.  $*p < 10^{-7}$  (unpaired Student's t-test,  $n=4$ , 10,000 cells counted per condition).
- (C) Dual positive cells were collected, fixed, and mounted. Direct visualization indicates a tau-YFP inclusion (white arrow) within an mCherry-expressing cell. Scale bar = 10  $\mu\text{m}$ .

## Discussion

We have tested the hypothesis that aggregated extracellular tau enters cells and transmits a misfolded state specifically to intracellular tau. We used recombinant MTBR tau prepared *in vitro* to form aggregates, which were readily taken up by cultured cells. Full-length tau-YFP protein does not readily aggregate within the cell, but internalized aggregates induce its fibrillization. When purified from cells, tau-YFP is competent to seed the fibrillization of tau monomer *in vitro*. Finally, we observed that aggregated intracellular tau transfers between co-cultured cells. We are uncertain how an aggregate taken into an endocytic vesicle might ultimately gain access to protein located in the cytoplasm, and whether aggregates that transfer from one cell to another are capable of inducing further intracellular aggregation. Aggregate uptake and induced aggregation in neighboring cells was recently suggested by co-culture of polyglutamine expressing cells, although this study failed to document direct transfer of aggregated protein (Ren et al. 2009). Relatively low efficiencies of cell-to-cell aggregate transfer and extracellular-to-intracellular seeding may make it difficult to document these events *in vitro*.

It is unknown why misfolded amyloid protein accumulates progressively throughout the brain in tauopathy and other neurodegenerative diseases. These data provide a plausible cellular mechanism, and are consistent with the hypothesis that tau aggregates propagate protein misfolding within the brain. Such aggregates could be released from dead or dying cells. Alternatively, they might move between cells via an exocytic process, as has been suggested for prion protein (Fevrier et al. 2004). Following uptake

by healthy neurons, the aggregates might stimulate further misfolding of an otherwise stable intracellular protein, in the manner of prions. The exocytosis model is more consistent with the observation that spread of tau pathology traditionally affects networks of neurons that are synaptically connected (Delacourte et al. 1999), though both mechanisms could act in concert to transfer tau aggregates between cells. These ideas await testing *in vivo*. We predict that introduction of exogenous fibrillar protein into the brain of a susceptible animal will induce further aggregation of endogenous protein and progressive pathology in a manner similar to prions.

We have recently shown that wild-type tau is capable of conformational diversity that depends on templated conformation change (Frost, Ollesch et al. 2009). These data, along with our present study, suggest a mechanism to explain disease-specific cellular vulnerabilities to misfolded protein based on fibrillization rate and propensity for propagation of a given misfolded species. Indeed, splicing variants or post-translational modifications of tau (e.g. phosphorylation) could render a subgroup of neurons particularly vulnerable to spontaneous or seeded protein misfolding. Thus the propagation of misfolded species through the brain would reflect a combination of neuronal proximity, connectivity, and the particular tau moieties expressed within the involved regions. Last, propagation via progressive, templated misfolding suggests a general pathogenic mechanism for other neurodegenerative diseases linked to amyloid protein aggregation.

## **CHAPTER 4**

# **THE EXPANDING REALM OF PRION PHENOMENA IN NEURODEGENERATIVE DISEASE**

# **The Expanding Realm of Prion Phenomena in Neurodegenerative Disease**

Bess Frost<sup>1,2,3</sup> and Marc I. Diamond<sup>1,2,3,4</sup>

From Departments of <sup>1</sup>Neurology, and <sup>2</sup>Cellular and Molecular Pharmacology,  
<sup>3</sup>Biomedical Sciences Program, and <sup>4</sup>Institute for Neurodegenerative Diseases  
University of California, San Francisco  
1600 16<sup>th</sup> St.  
San Francisco, CA  
Email: [marc.diamond@ucsf.edu](mailto:marc.diamond@ucsf.edu)

*[Accepted for publication in Prion April 16 2009]*

## **Abstract**

The aggregation of a soluble protein into insoluble,  $\beta$ -sheet rich amyloid fibrils is a defining characteristic of many neurodegenerative diseases, including prion disorders. The prion protein has so far been considered unique because of its infectious nature. Recent investigations, however, suggest that other amyloid-forming proteins associated with much more common diseases, such as tau,  $\alpha$ -synuclein, amyloid  $\beta$ , and polyglutamine proteins, while not infectious in the classical sense, share certain essential properties with prions that may explain phenotypic diversity, and patterns of spread within the nervous system. We suggest a common mechanism of pathogenesis of myriad sporadic and inherited neurodegenerative diseases based on templated conformational change.



## Templated Conformation Change and Phenotypic Diversity

The discovery of prions as a cause of sporadic, inherited, and infectious neurodegenerative disease has revolutionized our perspectives on mechanisms that underlie neurodegeneration. In each case, the disease relies on the conversion of the normal form of the prion protein, PrP<sup>C</sup>, to misfolded form, PrP<sup>Sc</sup> through a process termed “templated conformation change,” whereby a normally folded protein is converted to an abnormal conformation via direct contact with the misfolded species (Pan et al. 1993). This may involve other factors within the cell, but can occur *in vitro* with purified protein (Kocisko et al. 1994). Prion protein misfolding is likely balanced by cellular quality control pathways that degrade or help refold the polypeptide. If the balance tips toward accumulation, the PrP<sup>Sc</sup> load increases exponentially, and can cause a rapid neurodegenerative phenotype, although more chronic forms of degeneration are possible (Bessen et al. 1995; Telling et al. 1996; Prusiner 1997). PrP<sup>Sc</sup> can assemble into an assortment of structurally distinct species (Safar et al. 1998; Legname et al. 2006). Different PrP<sup>Sc</sup> conformers, or “strains,” generate different prion diseases, with characteristic progression rates and regions of pathology (Bessen et al. 1995). For example, Kuru, iatrogenic CJD, and variant CJD are caused by three conformationally distinct prion strains (Prusiner 1998).

The phenotypic diversity of prion disorders is mirrored by that of many other neurodegenerative diseases. For example, Parkinson disease (PD), dementia with Lewy bodies (Spillantini et al. 1997), and multiple system atrophy are all associated with

aggregation of  $\alpha$ -synuclein (Arima et al. 1998). Similarly, tau aggregation is occasionally seen in prionopathies (Ghetti et al. 1996) and synucleinopathies (Armstrong et al. 2005), and is the pathological hallmark in over twenty other neurodegenerative diseases, the tauopathies (Spillantini and Goedert 1998). Distinct fibrillar protein conformations thus could account for the phenotypic diversity in more common protein aggregation disorders. Conformational diversity and templated conformation change of wild-type protein has been described for three different neurodegenerative disease-associated proteins: tau, amyloid  $\beta$  ( $A\beta$ ), and  $\alpha$ -synuclein. Although not discussed here, evidence also supports this mechanism of pathogenesis for a variety of systemic amyloidoses (Walker et al. 2006).

*Tau.* The microtubule associated protein tau is the most common misfolded protein associated with human neurodegenerative diseases. Tau filament deposition in Alzheimer disease (AD), frontotemporal dementia, and other tauopathies correlates closely with cognitive dysfunction and cell death (Braak et al. 1991). Sporadic tauopathies involve only wild-type tau, and account for about 90% of tauopathy cases. Mutations in the tau gene cause various forms of frontotemporal dementia with Parkinsonism, termed FTDP-17 (Hutton et al. 1998; Poorkaj et al. 1998; Goedert et al. 2001). Tau mutations often result in increased rates of tau fibrillization and induce structurally distinct aggregates (von Bergen et al. 2000). Both sporadic and familial forms of tauopathy vary in brain region involvement, disease duration, age of onset, tau isoform expression, and fibril morphology (Buee et al. 2000). *In vitro* studies now indicate that wild-type tau monomer is capable of forming fibrils of various conformations that propagate via templated

conformational change, depending on the conformation on the initiating seed (Frost, Ollesch et al. 2009). These experiments demonstrate that tau aggregates, like prions, can exist in multiple, self-propagating conformations. Distinct wild-type tau conformers thus might underlie the myriad phenotypes of the tauopathies.

Conformational diversity of prions is reflected in the “species barrier,” which represents the inability of prions derived from different animals to cross-seed one another due to amino acid differences (Prusiner 1998). Species barriers block inter-species transmission in many cases, e.g. sheep to human, but can be overcome by an intermediate, such as cow, in the case of variant CJD (Prusiner 1998). Seeding barriers have recently been observed between different tau mutants. P301L mutant tau fibrils are unable to seed fibrillization of wild-type monomer, unlike fibrils formed from wild-type, R406W (Aoyagi et al. 2007), P301L/V337M double mutant (Frost, Ollesch et al. 2009), and  $\Delta$ K280 (Frost, Ollesch et al. 2009). This suggests that other amyloid proteins such as tau share fundamental characteristics of prions.

*A $\beta$* . Although it is typically conceived as a single disease, AD has been characterized as a heterogeneous spectrum of phenotypes (Armstrong et al. 2000). Much of this variation can be attributed to mutations in AD-associated proteins. Mutations in presenilin and the amyloid precursor protein (APP) cause early-onset AD, but age of onset and presence or absence of cerebral hemorrhage vary for a given APP mutation (Brouwers et al. 2008). Sporadic disease also exhibits variation in age of onset, rate of cognitive decline, and the location, presence and abundance of senile plaques and neurofibrillary tangles. *A $\beta$*

accumulation also occurs within myofibers to cause inclusion body myositis, a common age-related muscle disease (Askanas et al. 2006).

Distinct A $\beta$  conformers might help generate these disease subtypes. Wild-type A $\beta$  fibrils exhibit conformational diversity that is induced by varying growth conditions (Petkova et al. 2005). A $\beta_{1-40}$  fibrils prepared with or without gentle circular agitation form two different conformers, termed “quiescent” and “agitated.” Quiescent fibrils have a periodic twist, while agitated fibrils are straight and frequently paired. Based on solid-state nuclear magnetic resonance imaging, quiescent and agitated fibrils are also structurally distinct, and both fibril types propagate their conformations through serial seeding reactions. Quiescent fibrils are significantly more toxic to primary rat embryonic hippocampal neurons (Petkova et al. 2005). Thus A $\beta$  fibrils readily form conformationally distinct structures with unique cellular consequences. Further studies will be required to determine whether distinct pathologies *in vivo* can be linked to unique conformers.

*$\alpha$ -Synuclein.* Deposition of  $\alpha$ -synuclein into Lewy bodies occurs in many neurodegenerative diseases (Baba et al. 1998). Lewy bodies contain a dense core of filamentous and granular material surrounded by radially oriented fibrils, which are composed primarily of hyperphosphorylated  $\alpha$ -synuclein (Fujiwara et al. 2002). Missense mutations in  $\alpha$ -synuclein induce PD and dementia with Lewy bodies (Biskup et al. 2008). Like other amyloid-forming proteins,  $\alpha$ -synuclein is natively unstructured when prepared as a monomer *in vitro*, but forms  $\beta$ -sheet rich aggregates when incubated

at a high concentrations (Uversky et al. 2001). Alternatively, incubating  $\alpha$ -synuclein monomer with preformed wild-type or mutant (A30P) seeds induces its aggregation into distinct conformations (Wood et al. 1999) in a manner similar to tau (Frost, Ollesch et al. 2009; Yonetani et al. 2009). These distinct wild-type  $\alpha$ -synuclein aggregates differ in protease sensitivity, propensity for shedding, and immunoreactivity to different conformation-specific antibodies (Yonetani et al. 2009). As for tau and A $\beta$ , the conformational diversity of  $\alpha$ -synuclein may underlie or participate in the distinct clinical phenotypes of synucleinopathies.

*Mechanisms of phenotypic diversity.* It is clear that propagation of a fibrillar protein structure via templated conformation change is not unique to prion proteins. Future studies should help determine whether the structural diversity of these proteins underlies phenotypic diversity of the associated diseases *in vivo*. Detailed studies of the yeast prion, Sup35, have shed light on potential mechanisms by which fibrils of distinct conformations might affect the pathological phenotype. Like mammalian prions, Sup35 aggregates into  $\beta$ -sheet rich fibrils, which provide an epigenetic mode of inheritance (Patino et al. 1996). Aggregated Sup35 has reduced efficiency as a translation termination factor, its normal cellular role. By manipulating growth conditions, multiple synthetic phenotypes can be generated, reflected in colony pigment. The rate of fibril growth and fragility are key parameters in determining the strength of this phenotype, as the optimal rate of transmission of the Sup35 prion conformation to daughter cells depends on the ability to create a sufficient number of amyloid seeds (Tanaka et al. 2006). Recent work on mouse prion models also indicates that distinct PrP conformers

underlie variations incubation times, which correlates with sensitivity to urea denaturation (Legname et al. 2006). In other human amyloid diseases, phenotypic variation could derive from expression of specific splice isoforms or post-translational modifications of the target proteins, which would alter the propensity for initial misfolding, the conformation of the resultant fibril, and the efficiency of propagation.

## **Propagation of Misfolding**

All neurodegenerative diseases begin with dysfunction in a discrete brain region. For example, the first obvious signs of AD are memory loss derived from hippocampal dysfunction, whereas in PD the first prominent signs are a movement disorder due to degeneration of the substantia nigra. However, ultimately many neurodegenerative diseases spread to involve much larger areas of brain, along paths of neuronal proximity and connectivity. In tauopathies, tau aggregation along neuronal networks was described in the earliest studies (Arnold et al. 1991; Braak et al. 1991; Braak et al. 1997; Delacourte 1999). In AD brains, the distribution of neurofibrillary tangles correlates with neural connections, and vulnerability to degeneration correlates with distance from the affected areas (Arnold et al. 1991). If basic mechanisms of prion pathogenesis apply, then misfolded tau itself might spread neurodegeneration within the brain. A variety of independent studies now support this idea for tau and other amyloid-forming proteins.

Propagation of aggregation requires a misfolded protein in one cell to influence protein folding in an adjacent or connected cell. For example, PrP can travel from cell to cell in exosomes (Fevrier et al. 2004) and through tunneling nanotubes (Gousset et al. 2009). Although prions are infectious, since they can transmit between individuals, propagation of other types of protein misfolding within the brain would not require true “infectivity,” since the aggregates need only move between cells. Emerging data suggests that several types of protein aggregates are capable of entering cells, including

A $\beta$  (Magalhaes et al. 2005), polyglutamine (Yang et al. 2002), and tau (Frost, Jacks et al. 2009). However, detailed mechanisms of cell-cell spread are not yet known.

*Tau.* Tau is known principally as an intracellular protein: it binds, stabilizes and promotes the polymerization of neural microtubules (Weingarten et al. 1975). In disease, tau dissociates from microtubules and forms large, primarily intracellular,  $\beta$ -sheet rich fibrils. In tauopathy patients, extracellular tau is found as “ghost tangles” in the brain (Endoh et al. 1993), and in the cerebrospinal fluid (Vandermeeren et al. 1993). Emerging evidence suggests that tau levels in the CSF correlate with the risk of AD onset (Fagan et al. 2009). Extracellular tau aggregates, but not monomer, can enter cultured cells and stimulate fibrillization of intracellular tau, which is capable of further seeding of tau monomer *in vitro* (Frost, Jacks et al. 2009). Moreover, intracellular tau aggregates are capable of trans-cellular spread to co-cultured cells (Frost, Jacks et al. 2009). These data are consistent with tau aggregates being an agent of propagation *in vivo*.

*A $\beta$ .* Several lines of evidence suggest that exogenous A $\beta$  seeds can induce pathology in different animal models, consistent with templated conformational change. For example, marmosets express A $\beta$  with high sequence homology to humans. These animals develop A $\beta$  deposits in old age without developing AD. Injection of A $\beta$ -rich brain homogenates from patients with early-onset AD into these animals induces plaque formation within 6-7 years, but not in age-matched controls (Baker et al. 1994). Induction of A $\beta$  pathology from an exogenous seed has also been described in mice expressing APP, the holoprotein from which A $\beta$  is cleaved. In these mice, A $\beta$  deposition and A $\beta$  angiopathy develop with



age, or can be induced prematurely by injecting cortical extracts from either AD patients (Walker et al. 2002) or aged  $\beta$ APP mice (Meyer-Luehmann et al. 2006). Injecting these extracts into wild-type mice has no effect, and A $\beta$ -immunodepleted extracts fail to induce pathology. A $\beta$  aggregates formed *in vitro* and injected into mice have not been shown to induce pathology, suggesting that there may be cofactors present in brain extracts that confer transmissibility between animals. Alternatively, there may be a seeding barrier between *in vitro* prepared A $\beta$  aggregates and A $\beta$  monomer expressed *in vivo*. While there is no evidence that AD is transmissible between humans, these experiments show clear parallels between prion proteins and A $\beta$ .

*$\alpha$ -Synuclein.* Like tauopathies, synucleinopathies are temporally and anatomically progressive. Sporadic PD has been divided into six stages reflecting involvement of the entire brain, beginning with the medulla and spreading ultimately into the neocortex (Braak et al. 2003). Involvement of the substantia nigra occurs midway through this process, and brings patients to medical attention primarily because of the induced motor symptoms. Pathology beginning in the brainstem follows a principally upward course, ultimately reaching the neocortex. This is reminiscent of the spread observed in prion diseases and tauopathies, and raises the possibility that  $\alpha$ -synuclein pathology travels between neighboring or synaptically connected neurons (Braak et al. 2003). Indeed, recent studies of PD patients who received fetal mesencephalic dopaminergic neuron transplants describe the presence of ubiquitin and  $\alpha$ -synuclein-positive Lewy bodies in the engrafted neurons. Many of the deposits in the engrafted neurons were indistinguishable from lesions in the diseased host (Li et al. 2008). This suggests that

seeds from the surrounding diseased tissue may have spread into the graft to induce aggregation of native  $\alpha$ -synuclein.

## Summary

Non-infectious amyloid-forming proteins share many essential properties with prions. The conformational diversity of wild-type aggregates, and the capacity for propagation of these conformations via templated conformation change is shared by a growing number of amyloid-forming proteins. It remains to be determined whether such conformational diversity has pathologic correlates, as has been described for prions. The propagation of neurodegenerative diseases within the brain is also reminiscent of prion pathology. Extracellular aggregates can gain entry into cells, protein aggregates transfer between co-cultured cells, and exogenous aggregates can induce and spread pathology in animals. These data strongly suggest that protein aggregates in a variety of common sporadic and inherited neurodegenerative diseases can propagate misfolding from cell to cell. The emerging similarities between prions and other amyloid forming proteins will require further testing *in vivo* to determine physiologic relevance. If such commonalities truly underlie pathogenesis, it would suggest new therapeutic strategies to target transfer of aggregates between cells, and might also predict a limited utility of stem cell transplantation.

## **CHAPTER 5**

### **CONCLUSIONS AND FUTURE DIRECTIONS**

## Conclusions and Future Directions

Two curious aspects of tauopathies initiated our investigations into the prion-like characteristics of the microtubule-associated protein tau: 1) phenotypic diversity among the tauopathies, and 2) the inexplicable spread of disease through the brains of affected individuals (Delacourte 2005). These observations led to our hypothesis that wild-type tau is capable of conformational diversity driven by templated conformation change, and that tau aggregates propagate misfolding between cells.

We found that wild-type tau can be driven into alternative fibrillar conformations by two different mutant conformers, P301L/V337M and  $\Delta$ K280. Wild-type conformers differ in secondary structure, based on FTIR and CD, they differ in fragility, based on AFM and a quantitative CD-based fragility assay, and they differ morphologically, based on EM (Frost, Ollesch et al. 2009). These findings offer a theoretical framework with which to consider the diversity of sporadic tauopathies, which only involve wild-type tau. In patients, the stimuli that induce wild-type tau to form fibrils of a unique conformation could be myriad: splice isoforms, phosphorylation, a heterologous seed (e.g. A $\beta$ ), oxidation events, etc. In order to establish the *in vivo* relevance of these experiments, it is crucial to determine if tau conformers have distinct effects on cells, in mice, and in the brains of tauopathy patients.

In addition, we found that extracellular tau aggregates gain entry into cultured cells and co-localize with dextran, a marker of fluid-phase endocytosis. Once inside

cells, tau aggregates displace tubulin and induce fibrillization of transfected tau. Extracellularly-derived and intracellular tau aggregates co-localize with one another. Finally, aggregated intracellular tau is capable of transferring between co-cultured cells (Frost, Jacks et al. 2009). We predict that exogenous exposure to tau aggregates will initiate tau pathology in mouse models. In addition, mutant tau expressed in one area of the brain or in neural transplants containing tau aggregates should stimulate pathology in adjacent brain regions.

These prion-like characteristics of tau may provide additional therapeutic targets. It is of great clinical importance to determine the mechanism of aggregate uptake into cells and the method of cell-to-cell transfer. It is possible that blocking uptake or transfer between cells could stop the spread of tauopathy along neuronal networks in diseased patients.

## **APPENDIX A**

## **REFERENCES**

- Adachi, R., Yamaguchi, K., Yagi, H., Sakurai, K., Naiki, H. and Goto, Y. (2007). Flow-induced alignment of amyloid protofilaments revealed by linear dichroism. *J Biol Chem* 282(12): 8978-83.
- Akiyama, H., Barger, S., Barnum, S., Bradt, B., Bauer, J., Cole, G. M., Cooper, N. R., Eikelenboom, P., Emmerling, M., Fiebich, B. L., Finch, C. E., Frautschy, S., Griffin, W. S., Hampel, H., Hull, M., Landreth, G., Lue, L., Mrak, R., Mackenzie, I. R., McGeer, P. L., O'Banion, M. K., Pachter, J., Pasinetti, G., Plata-Salaman, C., Rogers, J., Rydel, R., Shen, Y., Streit, W., Strohmeyer, R., Tooyoma, I., Van Muiswinkel, F. L., Veerhuis, R., Walker, D., Webster, S., Wegrzyniak, B., Wenk, G. and Wyss-Coray, T. (2000). Inflammation and Alzheimer's disease. *Neurobiol Aging* 21(3): 383-421.
- Alzheimer, A. (1907). Uber eine eigenartige Erkrankung der Hirnrinde. *Allg Z Psychiat* 64:146-48.
- Aoyagi, H., Hasegawa, M. and Tamaoka, A. (2007). Fibrillogenic nuclei composed of P301L mutant tau induce elongation of P301L tau but not wild-type tau. *J Biol Chem* 282(28): 20309-18.
- Arima, K., Ueda, K., Sunohara, N., Arakawa, K., Hirai, S., Nakamura, M., Tonozuka-Uehara, H. and Kawai, M. (1998). NACP/alpha-synuclein immunoreactivity in fibrillary components of neuronal and oligodendroglial cytoplasmic inclusions in the pontine nuclei in multiple system atrophy. *Acta Neuropathol* 96(5): 439-44.
- Armstrong, R. A., Lantos, P. L. and Cairns, N. J. (2005). Overlap between neurodegenerative disorders. *Neuropathology* 25(2): 111-24.
- Armstrong, R. A., Nochlin, D. and Bird, T. D. (2000). Neuropathological heterogeneity in Alzheimer's disease: a study of 80 cases using principal components analysis. *Neuropathology* 20(1): 31-7.
- Arnold, S. E., Hyman, B. T., Flory, J., Damasio, A. R. and Van Hoesen, G. W. (1991). The topographical and neuroanatomical distribution of neurofibrillary tangles and neuritic plaques in the cerebral cortex of patients with Alzheimer's disease. *Cereb Cortex* 1(1): 103-16.
- Askanas, V. and Engel, W. K. (2006). Inclusion-body myositis: a myodegenerative conformational disorder associated with A $\beta$ , protein misfolding, and proteasome inhibition. *Neurology* 66(2 Suppl 1): S39-48.
- Asuni, A. A., Boutajangout, A., Quartermain, D. and Sigurdsson, E. M. (2007). Immunotherapy targeting pathological tau conformers in a tangle mouse model reduces brain pathology with associated functional improvements. *J Neurosci* 27(34): 9115-29.



- Baba, M., Nakajo, S., Tu, P. H., Tomita, T., Nakaya, K., Lee, V. M., Trojanowski, J. Q. and Iwatsubo, T. (1998). Aggregation of alpha-synuclein in Lewy bodies of sporadic Parkinson's disease and dementia with Lewy bodies. *Am J Pathol* 152(4): 879-84.
- Baker, H. F., Ridley, R. M., Duchen, L. W., Crow, T. J. and Bruton, C. J. (1994). Induction of beta (A4)-amyloid in primates by injection of Alzheimer's disease brain homogenate. Comparison with transmission of spongiform encephalopathy. *Mol Neurobiol* 8(1): 25-39.
- Bessen, R. A., Kocisko, D. A., Raymond, G. J., Nandan, S., Lansbury, P. T. and Caughey, B. (1995). Non-genetic propagation of strain-specific properties of scrapie prion protein. *Nature* 375(6533): 698-700.
- Biskup, S., Gerlach, M., Kupsch, A., Reichmann, H., Riederer, P., Vieregge, P., Wullner, U. and Gasser, T. (2008). Genes associated with Parkinson syndrome. *J Neurol* 255 Suppl 5: 8-17.
- Braak, E., Braak, H. and Mandelkow, E. M. (1994). A sequence of cytoskeleton changes related to the formation of neurofibrillary tangles and neuropil threads. *Acta Neuropathol* 87(6): 554-67.
- Braak, H. and Braak, E. (1991). Neuropathological staging of Alzheimer-related changes. *Acta Neuropathol (Berl)* 82(4): 239-59.
- Braak, H. and Braak, E. (1997). Frequency of stages of Alzheimer-related lesions in different age categories. *Neurobiol Aging* 18(4): 351-7.
- Braak, H., Del Tredici, K., Rub, U., de Vos, R. A., Jansen Steur, E. N. and Braak, E. (2003). Staging of brain pathology related to sporadic Parkinson's disease. *Neurobiol Aging* 24(2): 197-211.
- Brouwers, N., Sleegers, K. and Van Broeckhoven, C. (2008). Molecular genetics of Alzheimer's disease: an update. *Ann Med* 40(8): 562-83.
- Buee, L., Bussiere, T., Buee-Scherrer, V., Delacourte, A. and Hof, P. R. (2000). Tau protein isoforms, phosphorylation and role in neurodegenerative disorders. *Brain Res Brain Res Rev* 33(1): 95-130.
- Crowther, R. A. and Goedert, M. (2000). Abnormal tau-containing filaments in neurodegenerative diseases. *J Struct Biol* 130(2-3): 271-9.
- Cudkovicz, M., Qureshi, M. and Shefner, J. (2004). Measures and markers in amyotrophic lateral sclerosis. *NeuroRx* 1(2): 273-83.

- Delacourte, A. (1999). Biochemical and molecular characterization of neurofibrillary degeneration in frontotemporal dementias. *Dement Geriatr Cogn Disord* 10 Suppl 1: 75-9.
- Delacourte, A. (2005). Tauopathies: recent insights into old diseases. *Folia Neuropathol* 43(4): 244-57.
- Delacourte, A., David, J. P., Sergeant, N., Buee, L., Wattez, A., Vermersch, P., Ghazali, F., Fallet-Bianco, C., Pasquier, F., Lebert, F., Petit, H. and Di Menza, C. (1999). The biochemical pathway of neurofibrillary degeneration in aging and Alzheimer's disease. *Neurology* 52(6): 1158-65.
- DePace, A. H. and Weissman, J. S. (2002). Origins and kinetic consequences of diversity in Sup35 yeast prion fibers. *Nat Struct Biol* 9(5): 389-96.
- Endoh, R., Ogawara, M., Iwatsubo, T., Nakano, I. and Mori, H. (1993). Lack of the carboxyl terminal sequence of tau in ghost tangles of Alzheimer's disease. *Brain Res* 601(1-2): 164-72.
- Fagan, A. M., Head, D., Shah, A. R., Marcus, D., Mintun, M., Morris, J. C. and Holtzman, D. M. (2009). Decreased cerebrospinal fluid Abeta(42) correlates with brain atrophy in cognitively normal elderly. *Ann Neurol* 65(2): 176-183.
- Fevrier, B., Vilette, D., Archer, F., Loew, D., Faigle, W., Vidal, M., Laude, H. and Raposo, G. (2004). Cells release prions in association with exosomes. *Proc Natl Acad Sci U S A* 101(26): 9683-8.
- Friedhoff, P., von Bergen, M., Mandelkow, E. M., Davies, P. and Mandelkow, E. (1998). A nucleated assembly mechanism of Alzheimer paired helical filaments. *Proc Natl Acad Sci U S A* 95(26): 15712-7.
- Frost, B., Jacks, R. L. and Diamond, M. I. (2009). Propagation of tau misfolding from the outside to the inside of a cell. *J Biol Chem*.
- Frost, B., Ollesch, J., Wille, H. and Diamond, M. I. (2009). Conformational Diversity of Wild-type Tau Fibrils Specified by Templated Conformation Change. *J Biol Chem* 284(6): 3546-51.
- Fujiwara, H., Hasegawa, M., Dohmae, N., Kawashima, A., Masliah, E., Goldberg, M. S., Shen, J., Takio, K. and Iwatsubo, T. (2002). alpha-Synuclein is phosphorylated in synucleinopathy lesions. *Nat Cell Biol* 4(2): 160-4.
- Ghetti, B., Piccardo, P., Spillantini, M. G., Ichimiya, Y., Porro, M., Perini, F., Kitamoto, T., Tateishi, J., Seiler, C., Frangione, B., Bugiani, O., Giaccone, G., Prelli, F., Goedert, M., Dlouhy, S. R. and Tagliavini, F. (1996). Vascular variant of prion protein cerebral amyloidosis with tau-positive neurofibrillary tangles: the

- phenotype of the stop codon 145 mutation in PRNP. *Proc Natl Acad Sci U S A* 93(2): 744-8.
- Giasson, B. I., Forman, M. S., Higuchi, M., Golbe, L. I., Graves, C. L., Kotzbauer, P. T., Trojanowski, J. Q. and Lee, V. M. (2003). Initiation and synergistic fibrillization of tau and alpha-synuclein. *Science* 300(5619): 636-40.
- Goedert, M. and Jakes, R. (1990). Expression of separate isoforms of human tau protein: correlation with the tau pattern in brain and effects on tubulin polymerization. *Embo J* 9(13): 4225-30.
- Goedert, M., Spillantini, M. G., Serpell, L. C., Berriman, J., Smith, M. J., Jakes, R. and Crowther, R. A. (2001). From genetics to pathology: tau and alpha-synuclein assemblies in neurodegenerative diseases. *Philos Trans R Soc Lond B Biol Sci* 356(1406): 213-27.
- Gomez-Ramos, A., Diaz-Hernandez, M., Cuadros, R., Hernandez, F. and Avila, J. (2006). Extracellular tau is toxic to neuronal cells. *FEBS Lett* 580(20): 4842-50.
- Gomez-Ramos, A., Diaz-Hernandez, M., Rubio, A., Miras-Portugal, M. T. and Avila, J. (2008). Extracellular tau promotes intracellular calcium increase through M1 and M3 muscarinic receptors in neuronal cells. *Mol Cell Neurosci* 37(4): 673-81.
- Gousset, K., Schiff, E., Langevin, C., Marijanovic, Z., Caputo, A., Browman, D. T., Chenouard, N., de Chaumont, F., Martino, A., Enninga, J., Olivo-Marin, J. C., Mannel, D. and Zurzolo, C. (2009). Prions hijack tunnelling nanotubes for intercellular spread. *Nat Cell Biol* 11(3): 328-36.
- Greenberg, S. G. and Davies, P. (1990). A preparation of Alzheimer paired helical filaments that displays distinct tau proteins by polyacrylamide gel electrophoresis. *Proc Natl Acad Sci U S A* 87(15): 5827-31.
- Hofmann, M. W., Weise, K., Ollesch, J., Agrawal, P., Stalz, H., Stelzer, W., Hulsbergen, F., de Groot, H., Gerwert, K., Reed, J. and Langosch, D. (2004). De novo design of conformationally flexible transmembrane peptides driving membrane fusion. *Proc Natl Acad Sci U S A* 101(41): 14776-81.
- Hutton, M., Lendon, C. L., Rizzu, P., Baker, M., Froelich, S., Houlden, H., Pickering-Brown, S., Chakraverty, S., Isaacs, A., Grover, A., Hackett, J., Adamson, J., Lincoln, S., Dickson, D., Davies, P., Petersen, R. C., Stevens, M., de Graaff, E., Wauters, E., van Baren, J., Hillebrand, M., Joosse, M., Kwon, J. M., Nowotny, P., Che, L. K., Norton, J., Morris, J. C., Reed, L. A., Trojanowski, J., Basun, H., Lannfelt, L., Neystat, M., Fahn, S., Dark, F., Tannenberg, T., Dodd, P. R., Hayward, N., Kwok, J. B., Schofield, P. R., Andreadis, A., Snowden, J., Craufurd, D., Neary, D., Owen, F., Oostra, B. A., Hardy, J., Goate, A., van Swieten, J., Mann, D., Lynch, T. and Heutink, P. (1998). Association of missense and 5'-

- splice-site mutations in tau with the inherited dementia FTDP-17. *Nature* 393(6686): 702-5.
- Kanu, N., Imokawa, Y., Drechsel, D. N., Williamson, R. A., Birkett, C. R., Bostock, C. J. and Brookes, J. P. (2002). Transfer of scrapie prion infectivity by cell contact in culture. *Curr Biol* 12(7): 523-30.
- Kayed, R., Sokolov, Y., Edmonds, B., McIntire, T. M., Milton, S. C., Hall, J. E. and Glabe, C. G. (2004). Permeabilization of lipid bilayers is a common conformation-dependent activity of soluble amyloid oligomers in protein misfolding diseases. *J Biol Chem* 279(45): 46363-6.
- King, M. E., Kan, H. M., Baas, P. W., Erisir, A., Glabe, C. G. and Bloom, G. S. (2006). Tau-dependent microtubule disassembly initiated by prefibrillar beta-amyloid. *J Cell Biol* 175(4): 541-6.
- Kocisko, D. A., Come, J. H., Priola, S. A., Chesebro, B., Raymond, G. J., Lansbury, P. T. and Caughey, B. (1994). Cell-free formation of protease-resistant prion protein. *Nature* 370(6489): 471-4.
- Kosik, K. S., Joachim, C. L. and Selkoe, D. J. (1986). Microtubule-associated protein tau (tau) is a major antigenic component of paired helical filaments in Alzheimer disease. *Proc Natl Acad Sci U S A* 83(11): 4044-8.
- Lee, V. M., Goedert, M. and Trojanowski, J. Q. (2001). Neurodegenerative tauopathies. *Annu Rev Neurosci* 24: 1121-59.
- Legname, G., Nguyen, H. O., Peretz, D., Cohen, F. E., DeArmond, S. J. and Prusiner, S. B. (2006). Continuum of prion protein structures enciphers a multitude of prion isolate-specified phenotypes. *Proc Natl Acad Sci U S A* 103(50): 19105-10.
- LeVine, H., 3rd (1993). Thioflavine T interaction with synthetic Alzheimer's disease beta-amyloid peptides: detection of amyloid aggregation in solution. *Protein Sci* 2(3): 404-10.
- Levy, E., Carman, M. D., Fernandez-Madrid, I. J., Power, M. D., Lieberburg, I., van Duinen, S. G., Bots, G. T., Luyendijk, W. and Frangione, B. (1990). Mutation of the Alzheimer's disease amyloid gene in hereditary cerebral hemorrhage, Dutch type. *Science* 248(4959): 1124-6.
- Lewis, S. A., Wang, D. H. and Cowan, N. J. (1988). Microtubule-associated protein MAP2 shares a microtubule binding motif with tau protein. *Science* 242(4880): 936-9.
- Li, J. Y., Englund, E., Holton, J. L., Soulet, D., Hagell, P., Lees, A. J., Lashley, T., Quinn, N. P., Rehncrona, S., Bjorklund, A., Widner, H., Revesz, T., Lindvall, O.

- and Brundin, P. (2008). Lewy bodies in grafted neurons in subjects with Parkinson's disease suggest host-to-graft disease propagation. *Nat Med* 14(5): 501-3.
- Liu, W., Miller, B. L., Kramer, J. H., Rankin, K., Wyss-Coray, C., Gearhart, R., Phengrasamy, L., Weiner, M. and Rosen, H. J. (2004). Behavioral disorders in the frontal and temporal variants of frontotemporal dementia. *Neurology* 62(5): 742-8.
- Magalhaes, A. C., Baron, G. S., Lee, K. S., Steele-Mortimer, O., Dorward, D., Prado, M. A. and Caughey, B. (2005). Uptake and neuritic transport of scrapie prion protein coincident with infection of neuronal cells. *J Neurosci* 25(21): 5207-16.
- Masters, C. L., Simms, G., Weinman, N. A., Multhaup, G., McDonald, B. L. and Beyreuther, K. (1985). Amyloid plaque core protein in Alzheimer disease and Down syndrome. *Proc Natl Acad Sci U S A* 82(12): 4245-9.
- Meyer-Luehmann, M., Coomaraswamy, J., Bolmont, T., Kaeser, S., Schaefer, C., Kilger, E., Neuenschwander, A., Abramowski, D., Frey, P., Jaton, A. L., Vigouret, J. M., Paganetti, P., Walsh, D. M., Mathews, P. M., Ghiso, J., Staufenbiel, M., Walker, L. C. and Jucker, M. (2006). Exogenous induction of cerebral beta-amyloidogenesis is governed by agent and host. *Science* 313(5794): 1781-4.
- Miyasaka, T., Morishima-Kawashima, M., Ravid, R., Kamphorst, W., Nagashima, K. and Ihara, Y. (2001). Selective deposition of mutant tau in the FTDP-17 brain affected by the P301L mutation. *J Neuropathol Exp Neurol* 60(9): 872-84.
- Ollesch, J., Kunnemann, E., Glockshuber, R. and Gerwert, K. (2007). Prion protein alpha-to-beta transition monitored by time-resolved Fourier transform infrared spectroscopy. *Appl Spectrosc* 61(10): 1025-31.
- Ollesch, J., Poschner, B. C., Nikolaus, J., Hofmann, M. W., Herrmann, A., Gerwert, K. and Langosch, D. (2008). Secondary structure and distribution of fusogenic LV-peptides in lipid membranes. *Eur Biophys J* 37(4): 435-45.
- Pan, K. M., Baldwin, M., Nguyen, J., Gasset, M., Serban, A., Groth, D., Mehlhorn, I., Huang, Z., Fletterick, R. J., Cohen, F. E. and et al. (1993). Conversion of alpha-helices into beta-sheets features in the formation of the scrapie prion proteins. *Proc Natl Acad Sci U S A* 90(23): 10962-6.
- Patino, M. M., Liu, J. J., Glover, J. R. and Lindquist, S. (1996). Support for the prion hypothesis for inheritance of a phenotypic trait in yeast. *Science* 273(5275): 622-6.

- Petkova, A. T., Leapman, R. D., Guo, Z., Yau, W. M., Mattson, M. P. and Tycko, R. (2005). Self-propagating, molecular-level polymorphism in Alzheimer's beta-amyloid fibrils. *Science* 307(5707): 262-5.
- Poorkaj, P., Bird, T. D., Wijsman, E., Nemens, E., Garruto, R. M., Anderson, L., Andreadis, A., Wiederholt, W. C., Raskind, M. and Schellenberg, G. D. (1998). Tau is a candidate gene for chromosome 17 frontotemporal dementia. *Ann Neurol* 43(6): 815-25.
- Prusiner, S. B. (1997). Prion diseases and the BSE crisis. *Science* 278(5336): 245-51.
- Prusiner, S. B. (1998). Prions. *Proc Natl Acad Sci U S A* 95(23): 13363-83.
- Rafii, M. S. and Aisen, P. S. (2009). Recent developments in Alzheimer's disease therapeutics. *BMC Med* 7: 7.
- Ren, P. H., Lauckner, J. E., Kachirskaia, I., Heuser, J. E., Melki, R. and Kopito, R. R. (2009). Cytoplasmic penetration and persistent infection of mammalian cells by polyglutamine aggregates. *Nat Cell Biol*.
- Roberson, E. D., Scarce-Levie, K., Palop, J. J., Yan, F., Cheng, I. H., Wu, T., Gerstein, H., Yu, G. Q. and Mucke, L. (2007). Reducing endogenous tau ameliorates amyloid beta-induced deficits in an Alzheimer's disease mouse model. *Science* 316(5825): 750-4.
- Ryder, E. F., Snyder, E. Y. and Cepko, C. L. (1990). Establishment and characterization of multipotent neural cell lines using retrovirus vector-mediated oncogene transfer. *J Neurobiol* 21(2): 356-75.
- Safar, J., Wille, H., Itri, V., Groth, D., Serban, H., Torchia, M., Cohen, F. E. and Prusiner, S. B. (1998). Eight prion strains have PrP(Sc) molecules with different conformations. *Nat Med* 4(10): 1157-65.
- Sherrington, R., Rogaev, E. I., Liang, Y., Rogaeva, E. A., Levesque, G., Ikeda, M., Chi, H., Lin, C., Li, G., Holman, K. and et al. (1995). Cloning of a gene bearing missense mutations in early-onset familial Alzheimer's disease. *Nature* 375(6534): 754-60.
- Spillantini, M. G. and Goedert, M. (1998). Tau protein pathology in neurodegenerative diseases. *Trends Neurosci* 21(10): 428-33.
- Spillantini, M. G., Murrell, J. R., Goedert, M., Farlow, M. R., Klug, A. and Ghetti, B. (1998). Mutation in the tau gene in familial multiple system tauopathy with presenile dementia. *Proc Natl Acad Sci U S A* 95(13): 7737-41.

- Spillantini, M. G., Schmidt, M. L., Lee, V. M., Trojanowski, J. Q., Jakes, R. and Goedert, M. (1997). Alpha-synuclein in Lewy bodies. *Nature* 388(6645): 839-40.
- Tanaka, M., Chien, P., Naber, N., Cooke, R. and Weissman, J. S. (2004). Conformational variations in an infectious protein determine prion strain differences. *Nature* 428(6980): 323-8.
- Tanaka, M., Collins, S. R., Toyama, B. H. and Weissman, J. S. (2006). The physical basis of how prion conformations determine strain phenotypes. *Nature* 442(7102): 585-9.
- Telling, G. C., Parchi, P., DeArmond, S. J., Cortelli, P., Montagna, P., Gabizon, R., Mastrianni, J., Lugaresi, E., Gambetti, P. and Prusiner, S. B. (1996). Evidence for the conformation of the pathologic isoform of the prion protein enciphering and propagating prion diversity. *Science* 274(5295): 2079-82.
- Trinczek, B., Biernat, J., Baumann, K., Mandelkow, E. M. and Mandelkow, E. (1995). Domains of tau protein, differential phosphorylation, and dynamic instability of microtubules. *Mol Biol Cell* 6(12): 1887-902.
- Uversky, V. N., Li, J. and Fink, A. L. (2001). Evidence for a partially folded intermediate in alpha-synuclein fibril formation. *J Biol Chem* 276(14): 10737-44.
- Van Broeckhoven, C., Haan, J., Bakker, E., Hardy, J. A., Van Hul, W., Wehnert, A., Vegter-Van der Vlis, M. and Roos, R. A. (1990). Amyloid beta protein precursor gene and hereditary cerebral hemorrhage with amyloidosis (Dutch). *Science* 248(4959): 1120-2.
- Vandermeeren, M., Mercken, M., Vanmechelen, E., Six, J., van de Voorde, A., Martin, J. J. and Cras, P. (1993). Detection of tau proteins in normal and Alzheimer's disease cerebrospinal fluid with a sensitive sandwich enzyme-linked immunosorbent assay. *J Neurochem* 61(5): 1828-34.
- von Bergen, M., Friedhoff, P., Biernat, J., Heberle, J., Mandelkow, E. M. and Mandelkow, E. (2000). Assembly of tau protein into Alzheimer paired helical filaments depends on a local sequence motif ((306)VQIVYK(311)) forming beta structure. *Proc Natl Acad Sci U S A* 97(10): 5129-34.
- Walker, L. C., Callahan, M. J., Bian, F., Durham, R. A., Roher, A. E. and Lipinski, W. J. (2002). Exogenous induction of cerebral beta-amyloidosis in betaAPP-transgenic mice. *Peptides* 23(7): 1241-7.
- Walker, L. C., Levine, H., 3rd, Mattson, M. P. and Jucker, M. (2006). Inducible proteopathies. *Trends Neurosci* 29(8): 438-43.

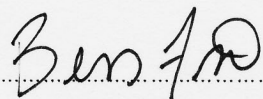
- Weingarten, M. D., Lockwood, A. H., Hwo, S. Y. and Kirschner, M. W. (1975). A protein factor essential for microtubule assembly. *Proc Natl Acad Sci U S A* 72(5): 1858-62.
- Wille, H., Govaerts, C., Borovinskiy, A., Latawiec, D., Downing, K. H., Cohen, F. E. and Prusiner, S. B. (2007). Electron crystallography of the scrapie prion protein complexed with heavy metals. *Arch Biochem Biophys* 467(2): 239-48.
- Wilson, D. M. and Binder, L. I. (1995). Polymerization of microtubule-associated protein tau under near-physiological conditions. *J Biol Chem* 270(41): 24306-14.
- Wischik, C. M., Novak, M., Thogersen, H. C., Edwards, P. C., Runswick, M. J., Jakes, R., Walker, J. E., Milstein, C., Roth, M. and Klug, A. (1988). Isolation of a fragment of tau derived from the core of the paired helical filament of Alzheimer disease. *Proc Natl Acad Sci U S A* 85(12): 4506-10.
- Wolfe, M. S., Xia, W., Ostaszewski, B. L., Diehl, T. S., Kimberly, W. T. and Selkoe, D. J. (1999). Two transmembrane aspartates in presenilin-1 required for presenilin endoproteolysis and gamma-secretase activity. *Nature* 398(6727): 513-7.
- Wood, S. J., Wypych, J., Steavenson, S., Louis, J. C., Citron, M. and Biere, A. L. (1999). alpha-synuclein fibrillogenesis is nucleation-dependent. Implications for the pathogenesis of Parkinson's disease. *J Biol Chem* 274(28): 19509-12.
- Yamaguchi, K., Takahashi, S., Kawai, T., Naiki, H. and Goto, Y. (2005). Seeding-dependent propagation and maturation of amyloid fibril conformation. *J Mol Biol* 352(4): 952-60.
- Yang, W., Dunlap, J. R., Andrews, R. B. and Wetzel, R. (2002). Aggregated polyglutamine peptides delivered to nuclei are toxic to mammalian cells. *Hum Mol Genet* 11(23): 2905-17.
- Yonetani, M., Nonaka, T., Masuda, M., Inukai, Y., Oikawa, T., Hisanaga, S. I. and Hasegawa, M. (2009). Conversion of wild-type alpha -synuclein into mutant-type fibrils and its propagation in the presence of A30P mutant. *J Biol Chem*.



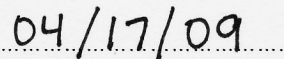
## PUBLISHING AGREEMENT

It is the policy of the University to encourage the distribution of all theses, dissertations, and manuscripts. Copies of all UCSF theses, dissertations, and manuscripts will be routed to the library via the Graduate Division. The library will make all theses, dissertations, and manuscripts accessible to the public and will preserve these to the best of their abilities, in perpetuity.

I hereby grant permission to the Graduate Division of the University of California, San Francisco to release copies of my dissertation to the Campus Library to provide access and preservation, in whole or in part, in perpetuity.



Susan "Bess" Frost



Date